STOCK ASSESSMENT OF THE SHORTFIN MAKO SHARK IN THE INDIAN OCEAN (IOTC), USING BAYESIAN SURPLUS PRODUCTION MODELS (JABBA): CATCH RECONSTRUCTION, DEMOGRAPHIC ANALYSIS, STOCK ASSESSMENT MODELS AND PROJECTIONS.

Rui Coelho[1,2,*], Daniela Rosa[1,2], Bruno Mourato[3]

SUMMARY

Bayesian Surplus Production Models were fitted to the Indian Ocean shortfin mako shark, using the JABBA framework (Just Another Bayesian Biomass Assessment). The catch history of the fishery used either the data reported to IOTC or, alternatively, a time series using estimated catches. Priors for the intrinsic growth rate of the population (r) were calculated using stochastic Leslie matrices, using a set of plausible life history parameters. An ensemble grid approach was used for the stock assessment, to incorporate uncertainties associated with the life history parameters and the form of the production function. The combination of the various scenarios used as the base case model grid ensemble showed that the stock is currently overfished (B<Bmsy) and subject to overfishing (F>Fmsy). Stochastic projections were carried out for this base case grid model ensemble. Given the current high levels of fishing mortality and stock status, there is a need to reduce future catches to a maximum value (TAC) of 40% of current catches, to prevent future declines in biomass and allow the population to start recovery.

KEYWORDS: Bayesian statistics, demographic analysis, Indian Ocean, JABBA, shortfin mako, stock assessment, surplus production models.

[1] Instituto Português do Mar e da Atmosfera (IPMA, I.P.), Av. 5 de Outubro s/n, 8700-305 Olhão, Portugal.

[2] Centro de Ciências do Mar (CCMAR), Universidade do Algarve, Campus de Gambelas, 8005-139 Faro, Portugal.

[3] Laboratório de Ciências da Pesca, Instituto do Mar, Universidade Federal de São Paulo (UNIFESP), Campus Baixada Santista, Brasil

* Corresponding author e-mail: rpcoelho@ipma.pt

Contents

1. Introduction

The shortfin mako is a pelagic shark species captured mostly as bycatch in oceanic pelagic fisheries worldwide, including in the Indian Ocean in the area under the jurisdiction of IOTC.

In 2018, the WPEB conducted a semi-quantitative Ecological Risk Assessment (ERA) to evaluate the resilience of sharks to the impact of IOTC fisheries, with the shortfin mako shark receiving the highest vulnerability ranking for longline gear (Murua et al., 2018, due to the very low productivity of the shortfin mako shark and its high susceptibility especially to pelagic longline gear.

Previous attempts have been made to assess the shortfin mako shark stock in the Indian Ocean. Specifically, a preliminary assessment was conducted in 2018 by Brunel et al. (2018) and another in 2020 by Bonhommeau et al. (2020). These assessments used catch-only models (CMSY) and biomass dynamic models (JABBA). Given the uncertainties at the time with regards to the stock status and lack of projections, the stock status of the shortfin mako shark in the IOTC remains "unknown".

In April 2024, a WPEB SMA data-preparatory meeting was held, where the WPEB agreed that the present year assessment should focus on the use of the biomass dynamic model based on the JABBA platform and, should time permit, other alternative models like CMSY could be explored. The WPEB also noted that using a grid approach over several variables would be appropriate, such as for exploring different life history options, CPUE scenarios and production functions, thus addressing both structural and estimation uncertainties.

The purpose of this paper is to present the stock assessment configuration, inputs and results for the IOTC shortfin mako shark. Specifically, we present the methods used and results regarding an alternative catch time series reconstruction, demographic analysis using Leslie matrices, stock assessment models configurations and results using JABBA, and stochastic projections, in order to provide management advice for this pelagic shark species to IOTC.

2. Material and methods

2.1. IOTC nominal catches and catch reconstructions

The IOTC nominal catch series was considered for the stock assessment. Some assumptions were made on this series, namely, to include all species codes in the IOTC database as being shortfin mako sharks for the following codes: MAK (mako sharks), MSK (sharks mackerel and porbeagles nei), SMA (shortfin mako), AG17 (mako sharks) and AG20 (sharks mackerel, porbeagles nei). By joining these codes some assumptions are made, particularly that for the generic code categories where more than one species can be included (i.e, MAK, MSK, AG17, AG20), the majority is composed by shortfin

mako (SMA). And given the impossibility to split those in the various species, all were considered and used as SMA.

It is important to note that with regards to those assumptions, that majority of the catch has been reported as either MAK (55,267.2 t) or SMA (47,515.0 t), while the remaining categories represent overall very small quantities (AG17: 115.9 t; AG20: 0.5 t and MSK: 1,601.5 t). As such, the main assumption made with this process was to assume that the MAK represents mostly shortfin mako shark. Given that the only other possible alternative is the longfin mako shark, which is in general a much rarer and occasionally species in oceanic fisheries, such assumption seems justifiable.

Additionally, an alternative catch series was used as a sensitivity analysis to the stock assessment, based on a catch reconstruction. The main methodology aspects used with this reconstruction are described in Murua et al. (2013) and have been updated to produce time-series data by Coelho et al. (2019). This method has been used in estimations presented and used as sensitivity analysis in ICCAT stock assessments (Coelho and Rosa, 2017), and in a preliminary IOTC SMA stock assessment (Brunel et al., 2018).

In terms of the methodology, and in summary, the catch reconstruction is carried out for all fleets and countries which are likely to be catching or bycatching sharks based on the ratio of shark catch or by-catch over the main target species of tuna and tuna-like species. The ratios are estimated through observer programmes when data is available, and in other cases from literature revisions and/or personal communications from national scientists (Murua et al., 2013).

The main assumption of the method is that the main target species (i.e., tunas and swordfish) reported by flag/fleet to the tuna-RFMOs are considered to be accurate, or at least more accurate than the sharks reportings, and it is therefore more reliable to use those target species quantities to calculate the likely shark catches or bycatches. Based on that, and assuming that each fleet uses a specific métier (i.e., gear characteristics and respective target species), the calculation based on ratios were then performed.

2.2. Life history and demographic analysis

There are biological and life history parameters available from previous studies for shortfin mako shark, including age and growth estimates, maximum age, age at maturity and fecundity. The parameters discussed by the WPEB at the data preparatory meeting and the decision on which ones to use are summarized in **Table 1**.

For the demographic analysis models, the age-specific fecundity was converted into female pup natality by multiplying the estimated fecundity-at-age by 0.5 (assumed as the proportion of female embryos in each litter, given a sex ratio of 1:1 for males:females). This value was then divided either by 2 or 3, depending on the assumption of a 2- or 3-year reproductive cycle for this species, a parameter that is still uncertain.

Natural mortality (M) was estimated with the use of several empirical equations that correlate different life history parameters with mortality. Those indirect estimations included both age-independent as well as age-dependent equations. The age-independent empirical equations used were the Pauly (1980) equation that uses Linf and k from the von Bertalanffy growth function (VBGF), the Hoenig (1983) equation that uses maximum observed ages, and the two Jensen (1996) equations that use age at maturity and k from the VBGF. The indirect methods using age-dependent equations were the Peterson and Wroblewski (1984) equation that estimates natural mortality as a function of weight at age, and the Chen and Watanabe (1989) equations that uses VBGF parameters to calculate age-specific natural mortality. Chen & Watanabe (1989) hypothesized that natural mortality in fish populations should have a U-shaped "bathtub" curve when plotted against age, and therefore proposed two equations: one describing falling mortality rates in early life stages/ages, and a second describing the increasing mortality towards later life stages/ages.

The various natural mortality estimates (M) obtained with the different methods were then used to calculate age-specific survivorship (S) using the equation: $S=e^{(-M)}$

The demographic analysis was carried out using age-structured Leslie matrices. Since only females produce offspring, the demographic analysis was carried out exclusively for the female components of the population (Simpfendorfer, 2004). The model considered a pre-breeding survey model type, where reproduction and natality take place first and only then survivorship-at-age probabilities are considered to act on the population.

Several different scenarios were considered for analysis and compared with the Leslie matrices, which are represented in **Table 2**. These scenarios accounted for different alternatives at the level of the growth equations (Liu et al., 2018; Takahashi et al., 2017) and fecundity, considering either 2- or 3-year reproductive cycles, which is still uncertain for the species (Mollet et al., 2002).

Considering that the two input vectors used in the Leslie matrices (i.e., age-specific fecundity and survivorship) have associated uncertainty errors, the Leslie matrices analysis were carried out using stochasticity in the input parameters. For the age-specific survivorship parameters, uncertainty was introduced by generating age-specific random values from a Triangular distribution, with limits defined between the age-specific minimum and maximum empirical estimations. For the fecundity parameters, uncertainty was incorporated by generating random age-specific fecundities following a Gaussian distribution with the expected value represented by the mean fecundity-at-age and the standard deviation represented by 0.25 of the mean.

The main parameter of interest that was estimated with the Leslie matrices demographic analysis is the population rate of increase (λ), calculated as the dominant eigenvalue of the projection matrix (Caswell, 2001). This value can then be converted to r (intrinsic population growth rate) with the equation: $r = \log(\lambda)$.

For comparison purposes, we further calculated steepness (*h*), using the equation h=â/(4+â), where â is the maximum lifetime reproductive rate which in turn is the product of R_0 (the net reproductive rate obtained from the Leslie matrix) and p_0, the survivorship at age 0, de from the empirical mortality estimates (Myers et al., 1999).

Each stochastic scenario was simulated 10,000 times by Monte Carlo Simulation. Each input parameter for each scenario was therefore randomly generated 10,000 times (based on the previously assumed distributions), and the 10,000 resulting Leslie matrices were compiled. The output parameters of the simulations were then analyzed and interpreted in terms of their mean and respective 95% confidence intervals (0.025 and 0.975 quantiles).

The Leslie matrix analysis was carried out in R (R Core Team, 2023), using libraries "primer" (Stevens, 2009), "popbio" (Stubben & Milligan, 2007) and "triangle" (Carnell, 2022).

Table 1: Life history parameters discussed by the WPEB for using in the IOTC assessment. The values agreed to be used are represented in bold.

Life History	Parameter	Value	Reference	NOTES/DECICION
Age and Growth	Linf (FL)	407.65	Barreto et al (2016) - Atlantic - Females (1 pair of bands/year)	
	k	0.04	Barreto et al (2016) - Atlantic - Females (1 pair of bands/year)	
	t0	-7.08	Barreto et al (2016) - Atlantic - Females (1 pair of bands/year)	
	Linf (FL)	441.64	Barreto et al (2016) - Atlantic - Females (2 pair of bands/year)	
	k	0.07	Barreto et al (2016) - Atlantic - Females (2 pair of bands/year)	
	t0	-3.98	Barreto et al (2016) - Atlantic - Females (2 pair of bands/year)	
	Linf (FL)	309.79	Barreto et al (2016) - Atlantic - Females (2 pair of bands/year up 5yr + 1 pair of bands/year thereafter)	
	k	0.13	Barreto et al (2016) - Atlantic - Females (2 pair of bands/year up 5yr + 1 pair of bands/year thereafter)	WPEB sugested to use either Liu et al. (2018) that is specific for IO, or Takahashi et al (2017) from a meta-analysis, due to uncertainties on the number of band pairs deposited per year.
	t0	-3.27	Barreto et al (2016) - Atlantic - Females (2 pair of bands/year up 5yr + 1 pair of bands/year thereafter)	
	Linf (FL)	350.3	Rosa et al (2017) - Atlantic - Females (1 pair of bands/year)	
	k	0.064	Rosa et al (2017) - Atlantic - Females (1 pair of bands/year)	
	t0	-3.09	Rosa et al (2017) - Atlantic - Females (1 pair of bands/year)	
	Linf (FL)	285.4	Groeneveld et al (2014) - IO, Sex comb (1 pair of bands/year)	
	k	0.113	Groeneveld et al (2014) - IO, Sex comb (1 pair of bands/year)	
	t0	-3.37	Groeneveld et al (2014) - IO, Sex comb (1 pair of bands/year)	
	Linf (FL)	**323.8**	Liu et al (2018) - IO - Females (1 pair of bands/year)	
	k	**0.075**	Liu et al (2018) - IO - Females (1 pair of bands/year)	
	t0	**-4.36**	Liu et al (2018) - IO - Females (1 pair of bands/year)	
	Linf (FL)	**321.044**	Takahashi et al (2017) Pacific - female (meta-analysis)	
	k	**0.128**	Takahashi et al (2017) Pacific - female (meta-analysis)	
	L0	**64.89**	Takahashi et al (2017) Pacific - female (meta-analysis)	
	t0	**-1.76**	Takahashi et al (2017) Pacific - female (meta-analysis) - Estimated from L0	
Lifespan	Tmax (years)	**32**	Natanson et al (2006)	Value for Atlantic
Reproduction	Size at maturity (FL)	**250**	Groeneveld et al (2014) - Females	Values mostly for the SW IO; WPEB noted the reproducitve cycle is uncertain, so agreed to test 2 and 3 years cycles
	Age at maturity (years)	**10.02**	Calculated from Takahashi et al (2017) growth	
	Age at maturity (years)	**15.36**	Calculated from Liu et al (2018) growth	
	Repro cycle (years)	**2 or 3**	Mollet et al (2000)	
	L0 - size at birth	**64.89**	Takahashi et al (2017) Pacific - female (meta-analysis)	
	Fecundity (pups)	**12**	Groeneveld et al (2014) (mean value, rounded)	
L-W relation	a	**0.0000349**	Romanov & Romanova (2009)	Values specific for IO
	b	**2.76544**		

Table 2: Scenarios built to be used in the demographic analysis, for determination of r priors for the stock assessment models. The values where the key differences exist for each scenario are represented in bold.

Parameters	Scenario 1	Scenario 2	Scenario 3	Scenario 4
	Liu et al (2018)		Takahashi et al (2017)	
Theoretical maximum length (FL)	**323.8**	**323.8**	**321.044**	**321.044**
Growth coefficient	**0.075**	**0.075**	**0.128**	**0.128**
Size at birth (FL)			64.89	64.89
Theoretical age at length zero	**-4.36**	**-4.36**	**-1.76**	**-1.76**
Size at 50% maturity (FL)	250	250	250	250
Mean age at 50% maturity (years)	**15**	**15**	**10**	**10**
Lifespan (years)	32	32	32	32
Sex ratio at birth	1:1	1:1	1:1	1:1
Reproductive cycle (years)	**3**	**2**	**3**	**2**
Litter size (pups)	12	12	12	12
Scalar coefficient of weight on length	0.0000349	0.0000349	0.0000349	0.0000349
Power coefficient of weight on length	2.76544	2.76544	2.76544	2.76544

2.3. Standardized CPUEs series

The CPUEs series that were originally available were those either available and/or presented at the IOTC WPEB data-preparatory meeting, and included series from the following CPCs/fleets/surveys (**Figure 1**):

- USSR historical surveys (1967-1989)
- Japan (1993-2018)
- Portugal (2000-2022)
- Spain (2001-2022)
- Taiwan (2005-2018), later replaced by Taiwan (2005-2022)

It is noted that after the WPEB data-preparatory meeting, Taiwan submitted an updated series with data until 2023 (Huynh and Tsai, 2023), that was further used as a sensitivity analysis in the stock assessment.

The CVs for each series in the models were those produced in the CPUE standardization analysis, except in cases where the values were lower than 0.2, in which cases a minimum CV of 0.2 was defined. This allowed some flexibility in the fit of the models to the CPUEs. All CPUEs were tested and considered in the models, and sensitivity models were run excluding one at a time, both in the full models containing all series as well in the base case models that were later defined for the stock assessment.
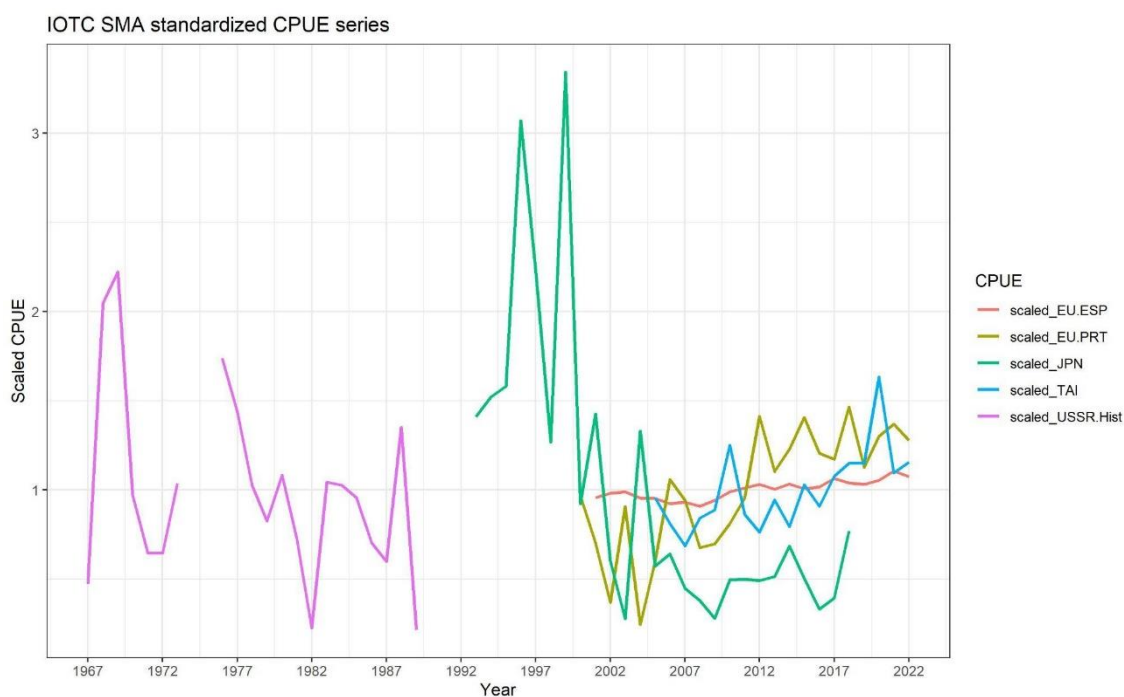
Figure 1: Standardized CPUE series available for the IOTC SMA stock assessment. For a better visualization and comparison, each series is scaled by its respective means.

2.4. Stock assessment

2.4.1. Assessment platform

The assessment models were implemented in JABBA, a Bayesian state-space surplus production model framework (Winker et al., 2018). JABBA is implemented in R and available from: github.com/jabbamodel/JABBA.

JABBA is a flexible Bayesian stock assessment modeling framework with various options, that include: 1) automatic fitting of multiple CPUE time series and associated standard errors, 2) estimating or fixing the process variance, 3) optional estimation of additional observation variance for individual or grouped CPUE time series 4) specifying the production function, i.e., Fox, Schaefer or Pella-Tomlinson, this last one by setting the inflection point from Bmsy/K and converting it into the shape parameter *m*, 5) setting priors for various parameters, including *r* and *K*, that can range from more to less informative depending on the confidence in the previously available information, 6) model diagnostics and goodness-of-fit features with associated tests and plots (e.g. residuals run tests, hindcast and retrospective analysis) and, 7) projections for constant catches (TACs) in the future to achieve management objectives over certain timeframes.

JABBA is implemented in R (R Core Team, 2023) and uses the JAGS software (Plummer, 2003) to estimate model parameters in a Bayesian framework, by means of Markov Chains Monte Carlo (MCMC) simulation. JAGS is executed from R using the library "r2jags" (Su and Yajima, 2012).

All analysis in this paper was conducted using R v.4.3.1. (R Core Team, 2023). Some additional libraries were used for manipulating and plotting data, including libraries "reshape" (Wickham, 2007), "doBy" (Højsgaard and Halekoh, 2023), "tidyr" (Wickham et al., 2023), "tidyverse" (Wickham et al., 2019), "ggplot2" (Wickham, 2016), "dplyr" (Wickham et al., 2023), "gridExtra" (Auguie, 2017) and "cowplot" (Wilke, 2024).

2.4.2. Stock assessment model specifications

The model specifications were based on an ensemble grid of models, given the current uncertainty that is associated with the shortfin mako sharks, not only in the Indian Ocean but elsewhere in general. The scenarios incorporate 2 main sources of uncertainty, set at the levels of 1) population growth parameters, which relate with the r priors and stock productivity, and 2) production functions, either Schaefer or variations of the Pella-Tomlinson model with the maximum of the production function set either below or above the Schaefer model, and which are related with assumptions in terms of density-dependence of the populations. The grid of models used is shown in **Table 3**.

For the Pella-Tomlinson models, the shape parameter (m) was estimated based on Bmsy/K, which were inputted in the models as informative priors set at 0.40 and 0.55, with a CV of 0.2, rather than as fixed values. This allowed some further variability to be included with the uncertainties associated with this parameter.

Two time series of catches were available, namely one with the data as reported to IOTC and another with estimated catches as described in this paper. Given that those time series have different values in terms of magnitude, it is difficult to include those options in the same model grid ensemble as the estimations of values such as B0 and MSY are dependent on the scale of the absolute values. As such, the base case grid of models was run using the catches reported to IOTC containing the assumptions mentioned previously, while a sensitivity analysis was carried out for using the estimated catches. The catches were used in the models with an associated CV of 0.2, therefore allowing some deviation from the observer catches to reflect the likelihood that the catches may not be accurately recorded and reported to IOTC.

In the model specifications, the K prior (carrying capacity) was kept as vaguely informative, given the lack of prior knowledge on these values and to allow for more emphasis to be put in the r parameter (intrinsic population growth rate), which is derived from biological data. Specifically, the K prior used the default settings of JABBA, namely the use of a lognormal prior with a large CV (100%) and a central value corresponding to 8 times the maximum total catch. This is consistent with other types of models, such as the approach used in catch-MSY (Martell and Froese, 2013).

For all models the same initial depletion (B_{1967}/K) was considered, using a prior with beta distribution with a mean of 0.9 and CV of 5%. Catchability parameters were formulated

as uninformative priors and the CPUEs were scaled externally by their respective means before inputting into the models.

The process error was defined by an uninformative inverse-gamma distribution with both the shape and scaling parameters set at 0.001 (see Gelman, 2006; used for e.g., by Mourato et al., 2023). Sensitivity analyses were carried out by fixing the sigma of the process error to CVs of 5% and 10%.

In addition to the CPUE variance associated with the data, the base case grid models configuration allowed the internal estimation of additional observation variance for each CPUE, allowing therefore for a larger divergence between the observed and model predicted CPUEs. A sensitivity analysis was carried out by disabling this process.

Table 3: Grid of ensemble JABBA models, used as the base case for the 2024 SMA IOTC stock assessment. Note that for the Pella-Tomlinson models the Bmsy/K values were used as priors and not as fixed values.

Variable	Grid options		
Catches	Reported		
CPUES	USSR, Japan, Spain		
Prod function	Pella (Bmsy/K=0.40)	Schaefer	Pella (Bmsy/K=0.55)
Productivity (r prior)	Lower (0.031)	Medium (0.055)	Higher (0.085)

For the parameter estimation in the Bayesian models, each MCMC chain was run with 50,000 iterations, used a burn-in period of 5,000 iterations, and a thinning rate of 5, reducing therefore the autocorrelation and dependence on the initial values. Each model specification was run for 3 independent chains, to better assess convergence and reduce any potential bias that might occur in a single chain analysis.

2.4.3. Model diagnostics

Basic diagnostics of model convergence included MCMC trace-plots and other statistics (Heidelberger and Welch, 1992; Geweke, 1992; Gelman and Rubin, 1992) implemented in the "CODA" package (Plummer et al., 2006).

To evaluate the CPUE fits, the model predicted CPUE indices were compared to the observed CPUE. Additionally, residual plots were used to examine the residuals of observed versus predicted CPUE indices for all fleets and boxplots with the median and quantiles of all residuals for each year (the area of each box indicates the strength of the discrepancy between CPUE series, with larger box indicating higher degree of conflicting information), and a loess smoother through all residuals to aid detection of the presence of systematic residual patterns.

Additionally, the root-mean-squared-error (RMSE) was used as a goodness-of-fit statistic, and runs tests were conducted to quantitatively evaluate the randomness of residuals (Carvalho et al., 2017). The runs test diagnostic was applied to residuals of the CPUE fit on log-scale considering the 2-sided p-value of the Wald-Wolfowitz runs test and is visualized in JABBA to illustrate which time series passed or failed the test, as well as highlighting individual data points that fall outside the three-sigma limits (Anhøj and Olesen, 2014).

To check for systematic bias in the stock status estimates, a retrospective analysis was carried out for all the base case Grid models. This analysis was carried out by sequentially removing one year of data at a time, over a total period of 4 years, and then refitting the model without those years. The parameters of interest (i.e., biomass, fishing mortality, B/Bmsy, F/Fmsy, B/K and MSY) were then compared to the original models fitted using the full time series. The presence of possible retrospective bias between the models was analyzed visually with plots, and statistically with the Mohn's rho (ρ) statistic (Mohn, 1999), using the formulation defined by Hurtado-Ferro et al. (2014). In this analysis, the more the values diverge from zero the stronger there is the presence of a retrospective bias. In general, values that fall between -0.15 and 0.2 are widely deemed as having an acceptable retrospective bias (Huerto et al., 2014).

The analysis included several sensitivity model runs, namely based on the following scenarios: 1) a catch only model without using information from the CPUE time series; 2) leave-one-out CPUE analysis where each CPUE was dropped at a time starting either with the full model using all available CPUEs or the base case model grid; 3) sensitivity analysis to the sigma of the process error (fixed at 5% and 10%) and inclusion of additional CPUE variance and; 4) a sensitivity analysis using the estimated catch time series. For the catch-only model, a prior was used for the terminal year depletion (B/K), set according to the values proposed by Kell et al. (2022), which are based on the ratio of the last year catches compared to the maximum catches over the time series.

For the sensitivity analysis, the base model Grid.02 was used, as this model uses a medium prior for *r*, and uses the Schaefer model that falls in the middle of the production curve from the 2 alternative Pella-Tomlinson models used, so it can be considered as a more central model from the base case grid of models.

2.5. Projections

The projections were conducted for the ensemble base case grid of models, with fixed catches ranging from 0% to 100% relative to current catches, with 10% increments. The current catches were defined as the average from the last 3 years of data (2020-2022). A 3-year lag in implementation was considered, given that the last year of data in the model is 2022, and the 1st year when a TAC can be implemented is 2026. This takes in consideration that the IOTC SC can adopt the management advice in 2024, and that the IOTC Commission can adopt the TACs in 2025 for implementation from 2026 onwards.

The projections were carried out for a period of 30 years given the long-life expectancy and low population growth dynamics of the shortfin mako sharks, and summarize the projected trajectories of B/Bmsy and F/Fmsy over time.

3. Results and Discussion

3.1. IOTC nominal catches and catch reconstructions

The time series of the IOTC reported catches versus the estimations using the ratio-based method are shown in **Figure 2**.

The two series have some differences in terms of absolute scale of values, but also in the shape of the historical catches. The nominal series peaks in 2014 at 5,359.7 t, while in that same year the estimated maximum potential catch is almost double, at 10,107.7 t. The main difference between the series is then in the trends for the subsequent years, when there is a decrease in the nominal IOTC catch series, while the estimated catches continue to increase until 2022. In the last terminal years, the differences are quite significant, namely 2,695.4 t for the IOTC reported catches versus 12,568.6 t for the ratio-based estimations.

One important note and assumption on the estimated SMA catches is that the fleets/métiers are identified based on catches of the main tuna and tuna-like species as reported to IOTC. Such data is based on the national reports from the national fisheries agencies, and can have significant limitations due to data collection, reporting efficiency and problems related with species identification. As such, those estimates are also affected by possible under- or non-reporting of the main targeted tuna and tuna like species by each country.

By the contrary, and especially for the more recent period, there is a possibility for a decrease in SMA catches, as seen in the official nominal IOTC data, due to recent restrictions that have been imposed by CITES and some national regulations. Given that the estimation method is based in the tuna and tuna-like main species (which excludes sharks), and as those main species are not in general subject to those specific shark regulations, for this more recent period there is the possibility that the shark catches of species like the shortfin mako using such ratios will be over-estimated.

It is therefore noted that this ratio-based method might no longer be fully applicable since the restrictions in shark catches and landings started to take place, and as such those estimations should be seen and handled with care. As such, those estimated catches were used mostly as a sensitivity analysis in the assessment.
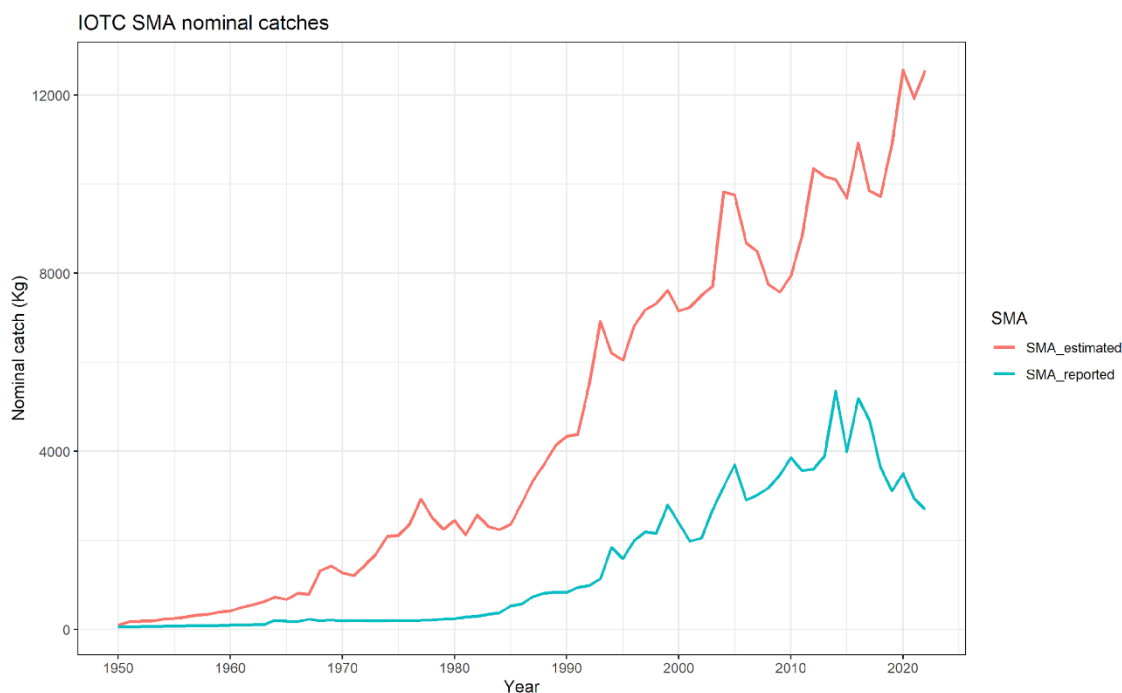
Figure 2: Time series of the SMA nominal catch data, both reported to IOTC and estimated using the methods described in Murua et al. (2013) and Coelho et al. (2019).

3.2. Life history and demographic analysis

The outputs from estimated intrinsic population growth rates (r) in each of the scenarios considered is summarized in **Figure 3**. The different scenarios reflect the variability associated with the different options for life history traits, as well as the uncertainty around both the fertility and age-specific survivorship, in this case derived from the natural mortality estimated from empirical equations. It is noted the two most contrasting scenarios, namely scenarios 1 and 4, with scenario 1 using slower growth rates from the VBGF (k) and a longer 3-year reproductive cycle, while scenario 4 uses a faster growth rate from the VBGF (k) and a shorter 2-year reproductive cycle. The scenarios 2 and 3 use a combination of both and fall in the middle of those.

It is important to emphasize that the estimated values for r range from point estimates of 0.031 to 0.085, which in all cases still represents very slow population growth rates, which seem fully aligned with the known life history traits of Lamniform sharks such as the shortfin mako. As a comparison, for the Atlantic (ICCAT) shortfin mako, Cortés (2017) obtained values of r ranging between 0.031-0.060 for the North Atlantic and between 0.066-0.123 for the South Atlantic, which are relatively similar and in line with those obtained here. In another work based on a global analysis, Yokoi et al. (2017) estimated a median r for the shortfin mako shark of 0.102, varying between 0.007 and 0.318. The median estimate of Yokoi et al (2017) is higher than our scenarios, but the ranges they produce include all our point estimates from our various scenarios.

For the South Pacific, (Huynh et al., 2022) estimated λ values between 1.098 and 1.063 year-1, considering either 2- or 3-year reproductive cycles, and using stage-based rather than age-based matrices. Our results include those values but have a wider dispersion, with the λ ranging between 1.021 and 1.107 year-1 (95% CIs limits of the distribution obtained from the 4 scenarios). In another analysis Tsai (2015) tested the influence of various assumption regarding the use of one vs two sex models, and provided λ estimates between 1.010 and 1.075, with an estimate of 1.047 year-1 for the model using females only, values which again fall within the range of estimates from our analysis.

Additionally, we also calculated steepness (h), which resulted in values ranging between 0.250 and 0.531 (95% CIs limits of the distribution obtained from the 4 scenarios). These values are again in line with the estimations of Cortes (2017) for the Atlantic, especially in the case of the North Atlantic where the h values ranged between 0.34 and 0.52, while for the South Atlantic ranged between 0.44 and 0.72.
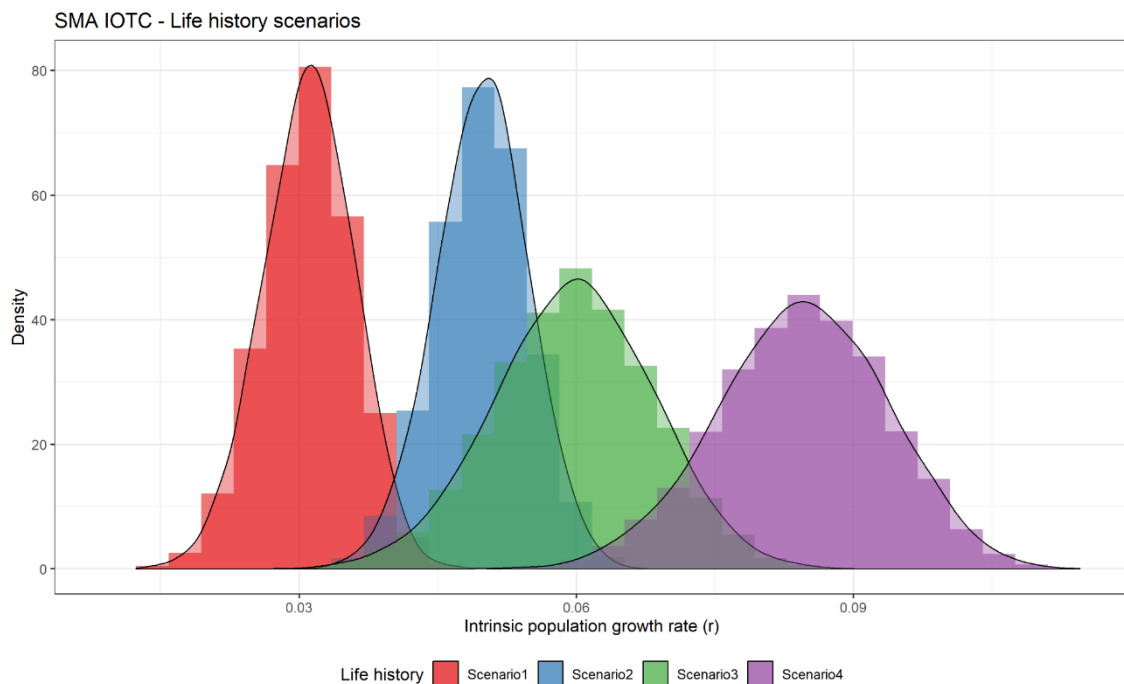

Figure 3: Distribution of r (intrinsic population growth rate) for the various scenarios based on the life history information for the shortfin mako shark, used in the 2024 IOTC stock assessment.

3.3. Stock assessment results

The stock assessment main results from the base case grid models, are summarized in **Table 4**.

The medians of the estimations of *K*, given by the marginal of the posterior distribution, ranged between 95,294.2 and 153,825.7 t. The values estimated for the posterior to prior median (PPMR) and variance (PPVR) ratios indicate that the *K* parameter has been informed by the data for all base case grid scenarios.

With regards to *r*, the medians of the marginal posteriors ranged between 0.032 and 0.089, with the values of PPMR and PPVR showing that the estimations were largely influenced by using informative priors for this parameter, as was expected. The initial depletion (psi) marginal posteriors for each scenario were also largely informed by the prior distribution relative to this ratio.

The range of *MSY* median estimates were relatively wide between the various grid models, ranging from 1,062.4 and 2,949.6 t, and had a median value of 1,873.1 t. The values of the absolute Bmsy ranged between 37,075.5 and 83,148.0 t, while the values of absolute Fmsy had a relatively narrow range with low values, between 0.013 and 0.079, as is expected for a species with a very low productivity as the shortfin mako shark.

Table 4: Summary of parameter estimates given by their posterior distributions, for the 2024 IOTC SMA stock assessment models. The quantiles presented represent the median for each parameter in each of the base case grid models, and the associated lower (LCI) and upper (UCI) bounds of the 95% credible intervals.

Parameter	GRID 01			GRID 02			GRID 03		
	Median	LCI	UCI	Median	LCI	UCI	Median	LCI	UCI
K	150743.6	80245.4	314265.0	130249.6	72616.4	266738.6	110224.4	64278.2	217573.6
r	0.032	0.024	0.043	0.057	0.043	0.077	0.089	0.066	0.120
psi	0.905	0.795	0.969	0.906	0.797	0.969	0.908	0.798	0.969
sigma.proc	0.118	0.046	0.195	0.115	0.050	0.195	0.106	0.042	0.190
m	2	2	2	2	2	2	2	2	2
Fmsy	0.016	0.012	0.021	0.029	0.021	0.038	0.045	0.033	0.060
Bmsy	75371.8	40122.7	157132.5	65124.8	36308.2	133369.3	55112.2	32139.1	108786.8
MSY	1209.3	607.0	2565.9	1873.1	998.0	3783.1	2455.6	1392.6	4793.8
Bmsy/K	0.500	0.500	0.500	0.500	0.500	0.500	0.500	0.500	0.500
B1967/K	0.888	0.670	1.103	0.893	0.677	1.103	0.899	0.692	1.103
B2022/K	0.418	0.199	0.793	0.442	0.199	0.822	0.511	0.234	0.874
B2022/Bmsy	0.836	0.397	1.585	0.885	0.399	1.643	1.023	0.469	1.749
F2022/Fmsy	2.727	0.969	6.751	1.672	0.600	4.088	1.120	0.396	2.719

Parameter	GRID 07			GRID 08			GRID 09		
	Median	LCI	UCI	Median	LCI	UCI	Median	LCI	UCI
K	142798.5	77955.8	278344.1	117890.4	68424.2	228819.9	95294.2	59048.5	175821.7
r	0.032	0.024	0.043	0.057	0.043	0.077	0.089	0.066	0.120
psi	0.905	0.796	0.968	0.905	0.796	0.968	0.907	0.798	0.970
sigma.proc	0.117	0.051	0.195	0.112	0.043	0.193	0.114	0.044	0.193
m	1.14	0.77	1.68	1.13	0.77	1.67	1.12	0.77	1.65
Fmsy	0.028	0.017	0.046	0.051	0.031	0.083	0.079	0.049	0.127
Bmsy	55820.0	29386.7	111922.8	46184.5	25424.1	94034.4	37075.5	21557.9	72440.7
MSY	1583.2	782.2	3180.0	2365.3	1289.6	4481.4	2949.6	1777.0	5274.8
Bmsy/K	0.392	0.321	0.467	0.391	0.321	0.465	0.389	0.320	0.463
B1967/K	0.885	0.662	1.101	0.891	0.680	1.102	0.896	0.683	1.105
B2022/K	0.419	0.189	0.780	0.445	0.203	0.807	0.465	0.221	0.801
B2022/Bmsy	1.070	0.479	2.021	1.140	0.516	2.102	1.199	0.558	2.113
F2022/Fmsy	1.650	0.581	4.379	1.033	0.363	2.621	0.785	0.273	1.949

Parameter	GRID 19			GRID 20			GRID 21		
	Median	LCI	UCI	Median	LCI	UCI	Median	LCI	UCI
K	153825.7	78895.7	363392.8	137008.1	74546.3	307261.1	113563.5	63469.2	233681.5
r	0.032	0.024	0.043	0.057	0.042	0.077	0.089	0.066	0.120
psi	0.904	0.795	0.969	0.906	0.799	0.969	0.908	0.801	0.970
sigma.proc	0.121	0.050	0.197	0.111	0.043	0.193	0.106	0.032	0.191
m	2.50	1.68	3.73	2.47	1.66	3.65	2.43	1.65	3.59
Fmsy	0.013	0.008	0.021	0.023	0.014	0.038	0.037	0.022	0.061
Bmsy	83148.0	41791.4	198520.7	73579.2	39352.2	169643.8	60999.6	32882.1	129866.3
MSY	1062.4	489.6	2555.8	1721.8	854.7	3885.1	2254.7	1173.9	4563.8
Bmsy/K	0.543	0.467	0.617	0.541	0.464	0.614	0.538	0.463	0.610
B1967/K	0.885	0.662	1.107	0.895	0.682	1.102	0.901	0.686	1.102
B2022/K	0.410	0.160	0.807	0.467	0.184	0.865	0.512	0.227	0.865
B2022/Bmsy	0.759	0.294	1.503	0.866	0.337	1.619	0.955	0.419	1.636
F2022/Fmsy	3.443	1.226	9.197	1.867	0.629	4.882	1.313	0.437	3.403

3.4. Model validation

The MCMC convergence tests by Heidelberger and Welch (1992) and Geweke (1992) all passed with regards to the MCMC estimation of the parameters for all models. An adequate convergence of the MCMC chains was also corroborated visually by checking the trace plots, which showed good mixing and random deviations around the parameters

space, without any detectable bias or patterns that could result from autocorrelations in the estimations.

The fits of the base case grid models to each of the 3 standardized CPUE indices used for those final models are shown in **Figure 4**. The goodness-of-fit of those residuals were similar between all base case grid models used, with the RMSE statistic ranging between 45.7% and 47.3% (**Figure 5**).

The runs test for those CPUE residuals from each of the grid models are provided in **Figure 6**. Only one CPUE series passed the runs tests for all models, namely the historical USSR series. The Japanese series passed in some of the grid models and failed in others, while the Spanish CPUE showed patterns of non-randomness in the residuals. Additionally, some outliers were also identified in the residuals, defined as points outside a 3-fold limit around the overall residuals means (Anhøj and Olesen, 2014).

The deviations from the process error show similar patterns for all base case grid models, with the deviates centered around zero and with the 95% credibility intervals always including the zero value during the entire time series (**Figure 7**). This suggests that there is no major evidence of structural model misspecifications.

The results of the retrospective analysis applied to all the base case grid models are shown in **Figure 8,** and the corresponding summaries of the estimations of the Mohn's rho are summarized in **Table 5**. All base case grid models fell within the acceptable range of -0.15 to 0.20, as defined by Hurtado-Ferro et al. (2014) and Carvalho et al. (2017), relative to all parameters from the various stock quantities. This analysis confirms that, in general, there are no major retrospective patterns in the models.

The hindcast cross-validation procedure was conducted mostly for the index where data for the last years was available, namely for Spain. The results show that the predictions when 1-year at a time for the last 4-years, all fall within the limits of the 95% CIs (**Figure 9**). Nonetheless, the mean absolute scaled error (MASE) estimates were above the reference level (MASE > 1), indicating that the average forecasts for this index have poor predictive skills (Carvalho et al., 2021) and there was a pattern for the predictions to be always under the observed values as the various consecutive years were removed.

On the other hand, hindcast cross-validation was also conducted for the index from Japan, but in that case with models terminating in 2018, as that was the last year when the index is available (**Figure 10**). In this case the results also show that the predictions fall inside the limits of the 95% CIs, and the estimates are within the reference level (MASE < 1), indicating that the average forecasts for this index have good predictive skills.
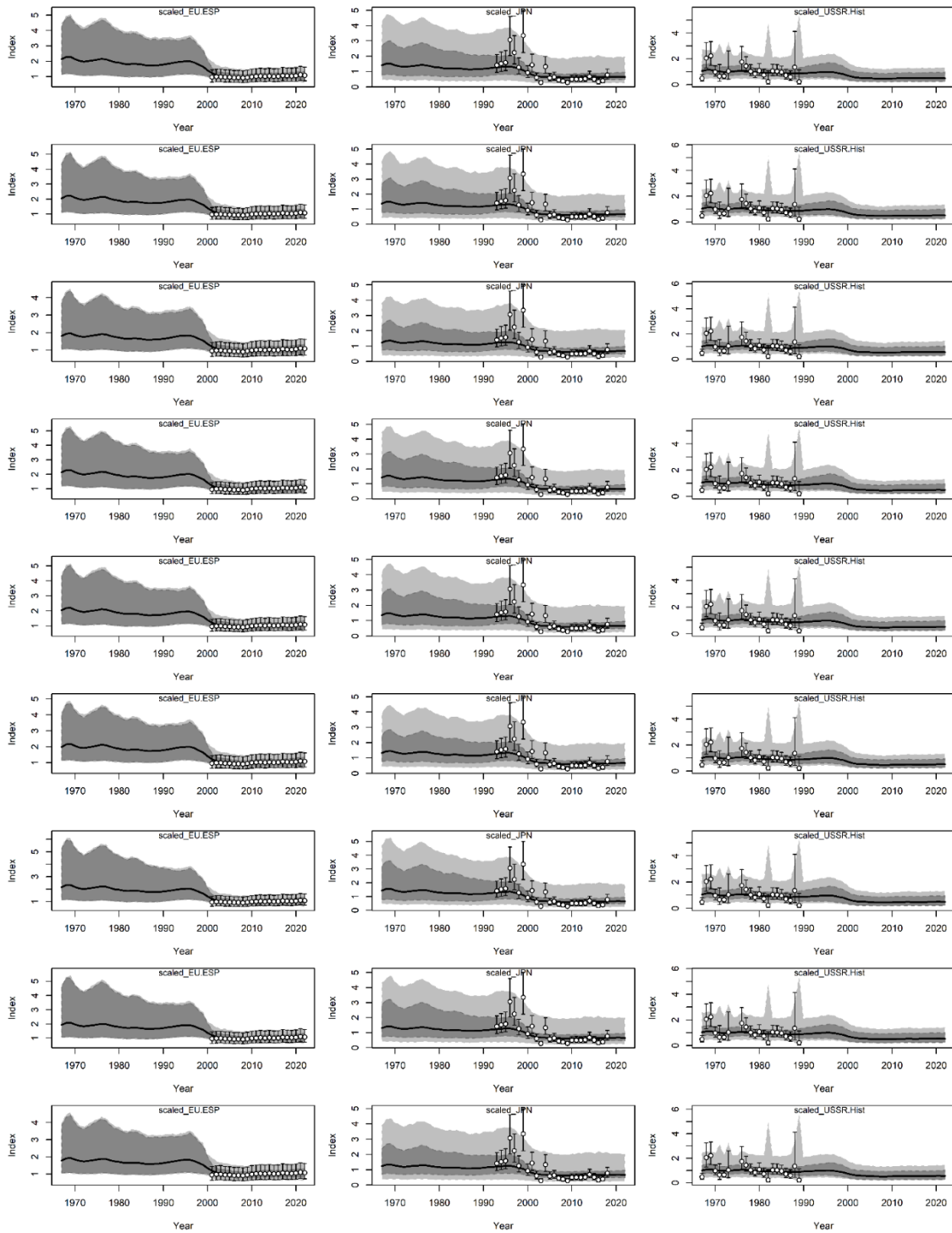
Figure 4: Time series of observed (circles) and predicted (solid line) CPUEs for the IOTC SMA stock assessment models, for each base case grid model. The dark shaded areas represent the 95% credibility intervals of the expected mean CPUE, and the light shaded areas represent the 95% posterior predictive distribution intervals. The error bars are the 95% confidence intervals (CIs) from the CPUE observations.
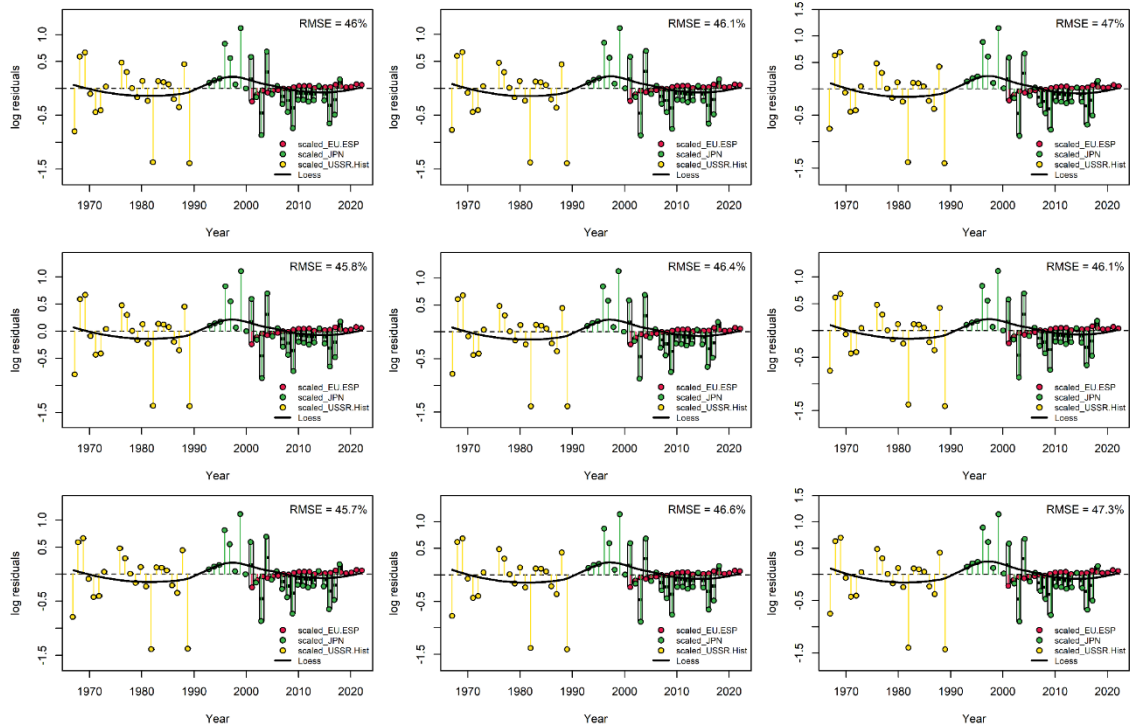
Figure 5: Residuals diagnostic plots for the base case grid models run for the 2024 IOTC SMA stock assessment. Each individual CPUE index and its respective residuals are represented by a different color. The solid black lines represent loess smoothers through all residuals combined.
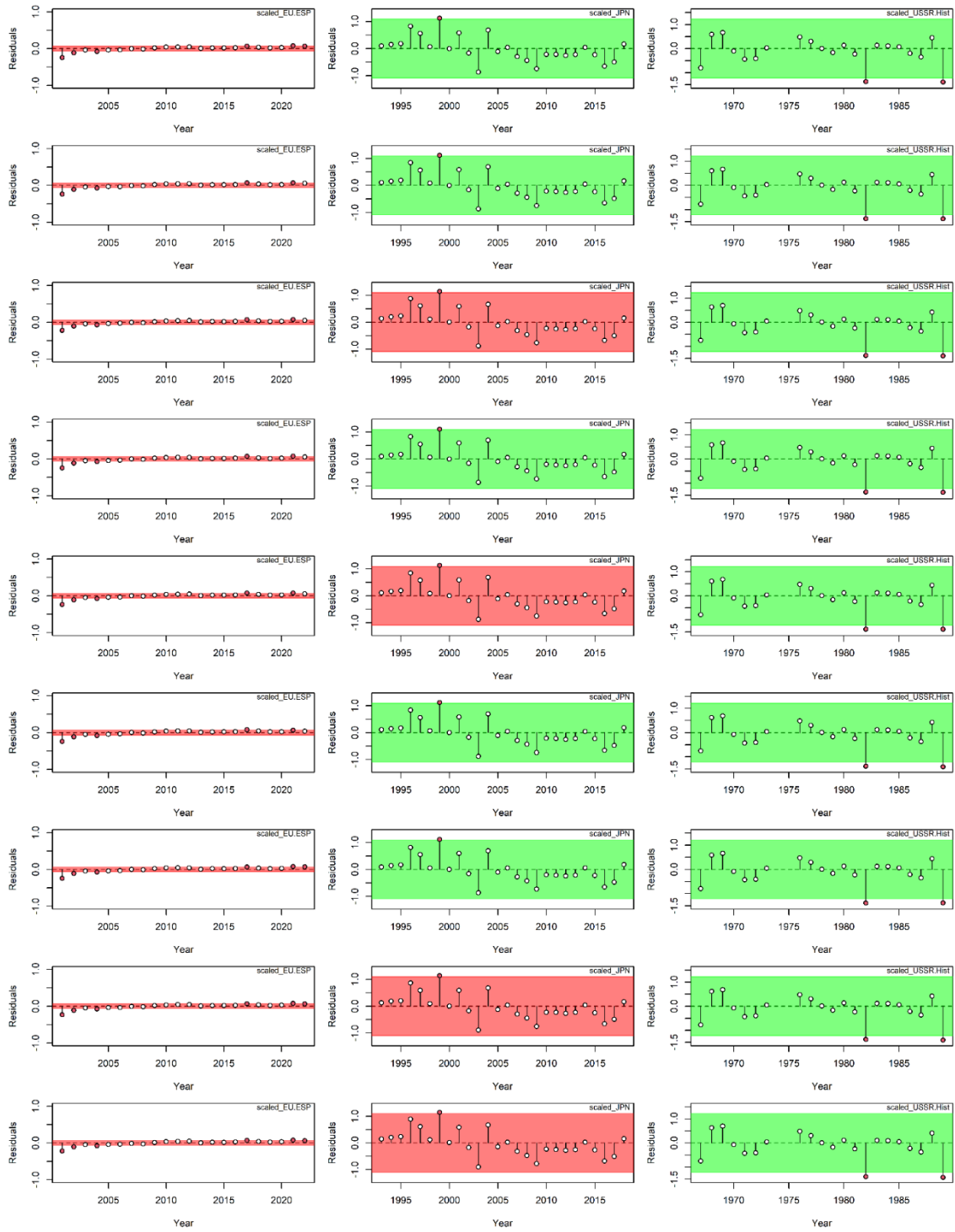
Figure 6: Runs tests for the CPUE index for all the base case grid models, used for the 2024 IOTC SMA stock assessment.
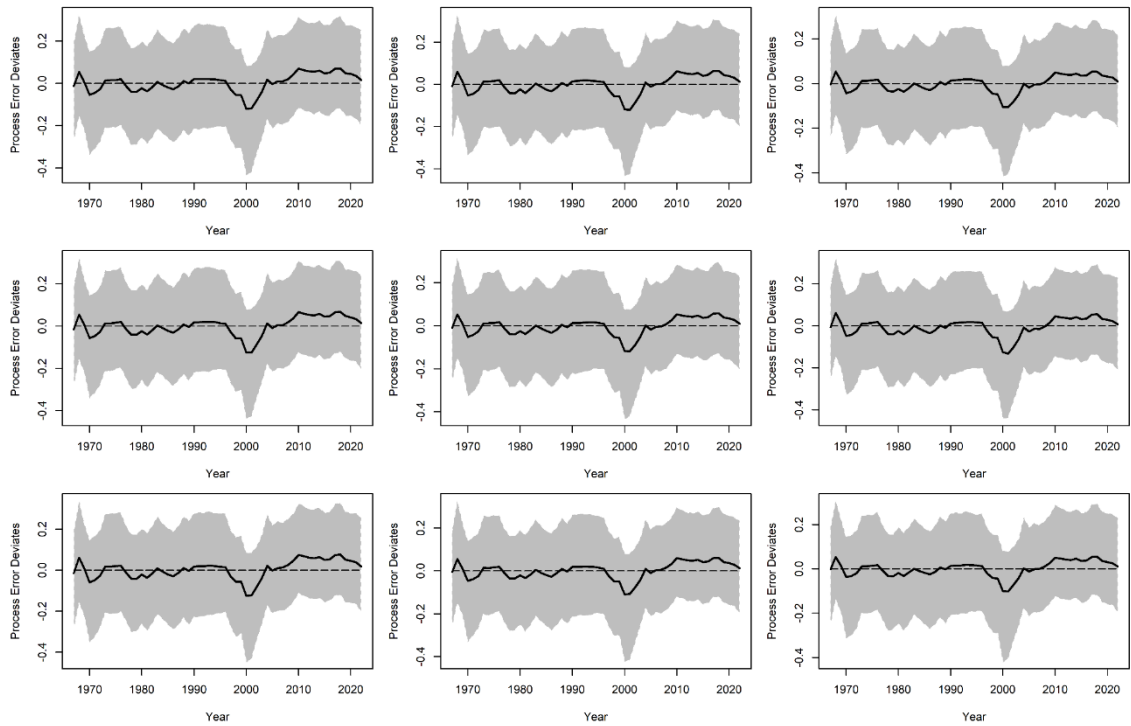
Figure 7: Process error deviates for the base case grid models for the 2024 IOTC SMA stock assessment. The solid line represents the median, and the shaded gray area the 95% credibility intervals.
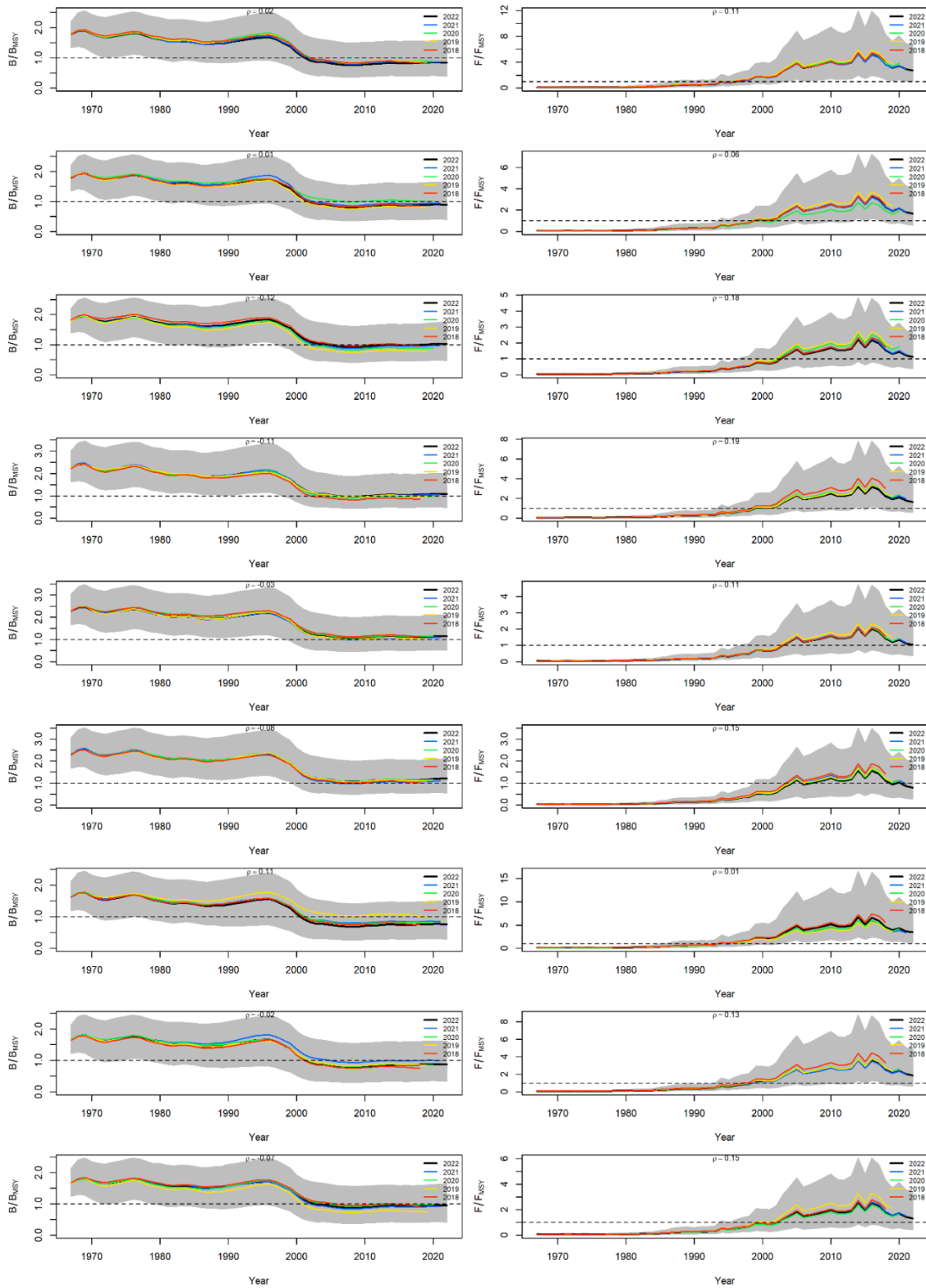
Figure 8: Retrospective analysis conducted for all base case grid models for the 2024 IOTC SMA stock assessment, by removing 1-year at a time sequentially (n=4) and predicting the trends in biomass and fishing mortality relative to MSY (i.e, B/Bmsy and F/Fmsy).

Table 5: Summary of the Mohn's rho statistic computed from the retrospective analysis pattern evaluated for the base case Grid models. Values that fall between -0.15 and 0.2 are considered as having an acceptable retrospective bias (Huerto et al., 2014), and are highlighted in green in this table.

Model	B	F	Bmsy	Fmsy	B/K	MSY
Grid.1	-0.08	0.11	0.02	0.11	-0.02	-0.10
Grid.2	-0.03	0.06	0.01	0.06	-0.02	-0.05
Grid.3	-0.14	0.18	-0.12	0.18	-0.02	-0.03
Grid.7	-0.14	0.18	-0.11	0.19	-0.02	-0.05
Grid.8	-0.08	0.11	-0.03	0.11	-0.01	-0.05
Grid.9	-0.12	0.15	-0.08	0.15	-0.01	-0.07
Grid.19	0.02	0.00	0.11	0.01	-0.03	-0.05
Grid.20	-0.09	0.12	-0.02	0.13	-0.01	-0.11
Grid.21	-0.09	0.14	-0.07	0.15	-0.01	-0.05
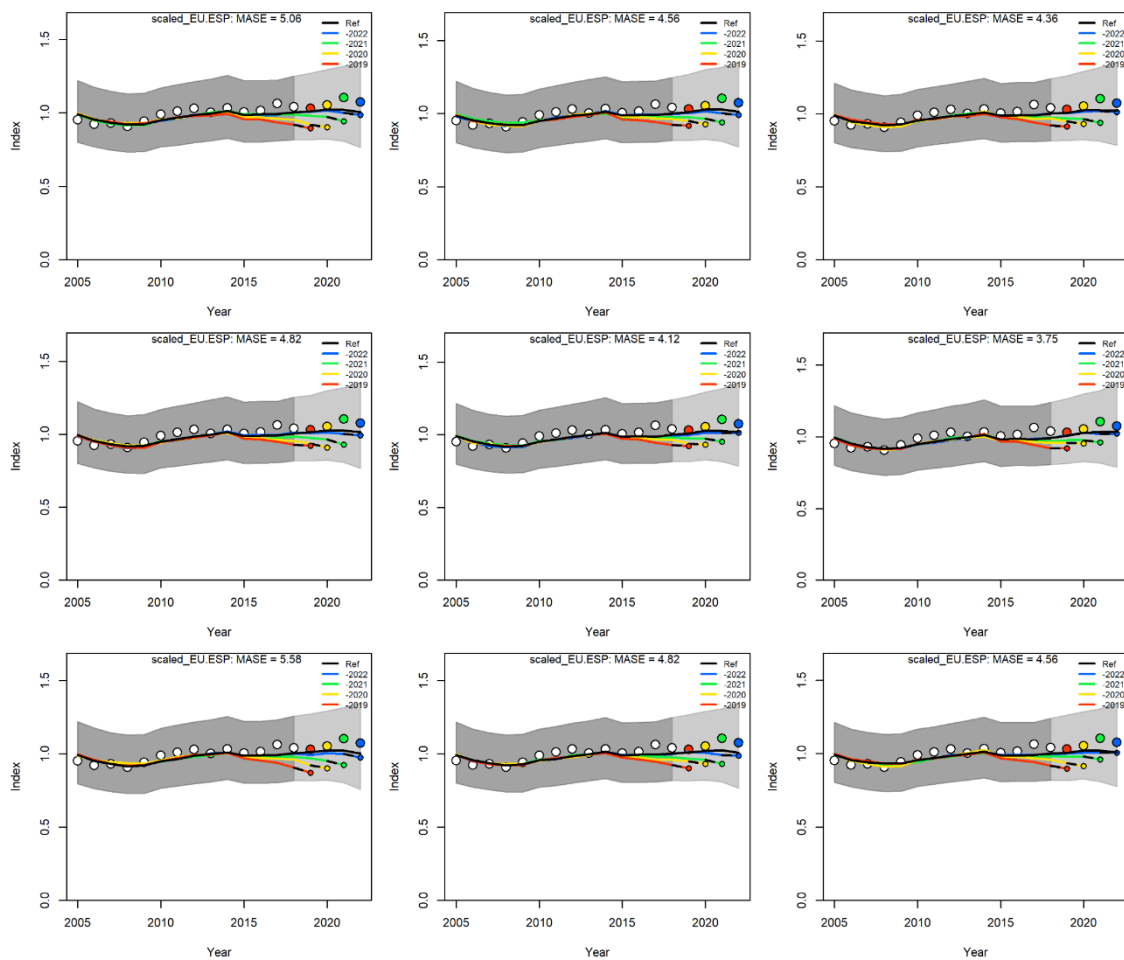
Figure 9. Hindcasting cross-validation results for the index available in the last years of the model (Spain), run for all base case grid models in the 2024 SMA IOTC stock assessment. The plots show 1-year-ahead forecasts of CPUE values (2019-2022) when the last years are removed one at a time, relative to the observed CPUE using all data.

The CPUE observations, used for cross-validation are highlighted as the color-coded solid circles with associated light-grey shaded 95% confidence interval.
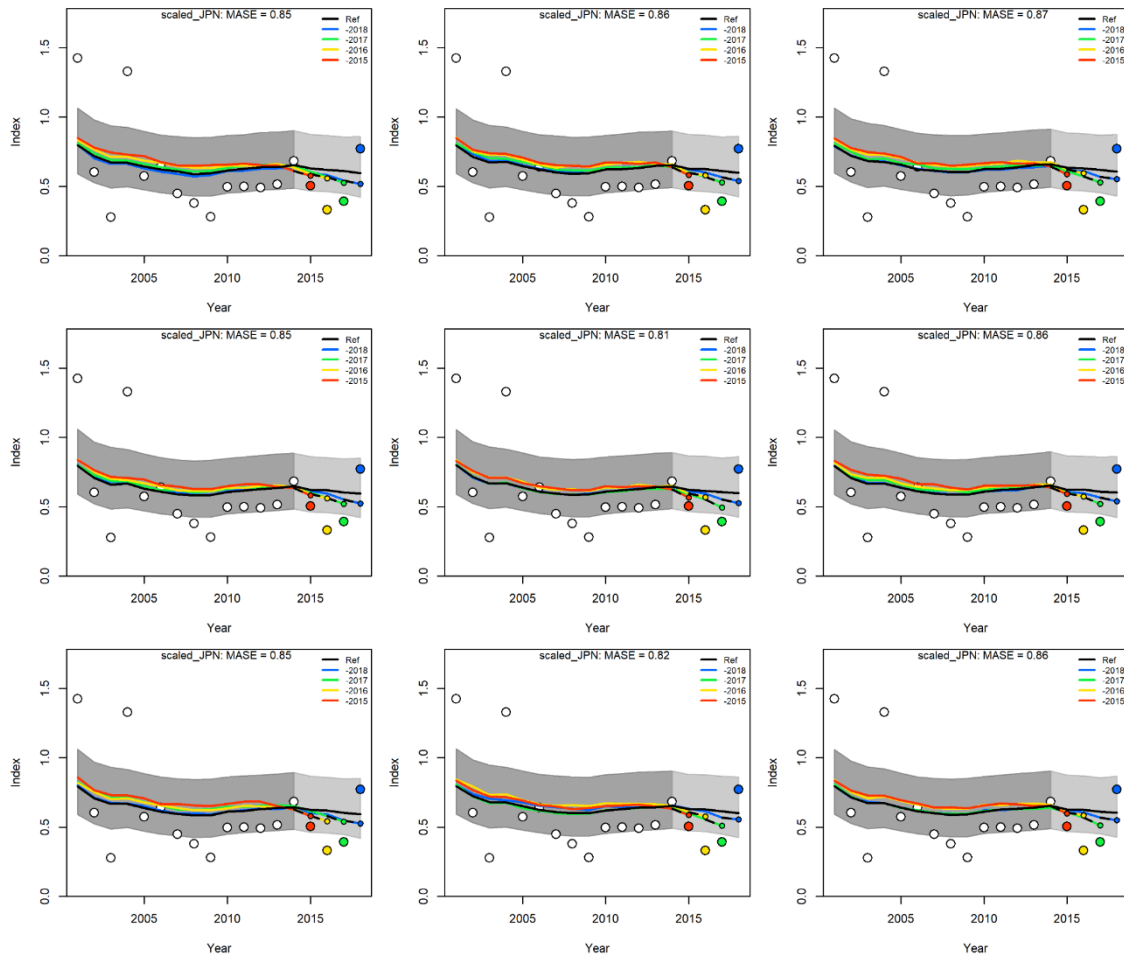

Figure 10. Hindcasting cross-validation results for the index from Japan, with models terminating in 2018, the last year when that index is available. The plots show 1-year-ahead forecasts of CPUE values (2015-2018) when the last years are removed one at a time, relative to the observed CPUE using all data. The CPUE observations, used for cross-validation are highlighted as the color-coded solid circles with associated light-grey shaded 95% confidence interval.

3.5. Sensitivity analysis

3.5.1. Catch only model

The results of the sensitivity analysis conducted for a model with catch only information is shown in **Figure 11**. It is noted a very distinct behavior when the CPUE data is entirely excluded, and the results are mostly informed by the biological prior information, the priors set for initial and final depletion, and the history and trends from the times series of the catches. In general, the biomass trends using only the catch information start to

decline by around 2000, and continue to continuously decline over the time series. This results in a very pessimistic final scenario, where the stock would be much more depleted.
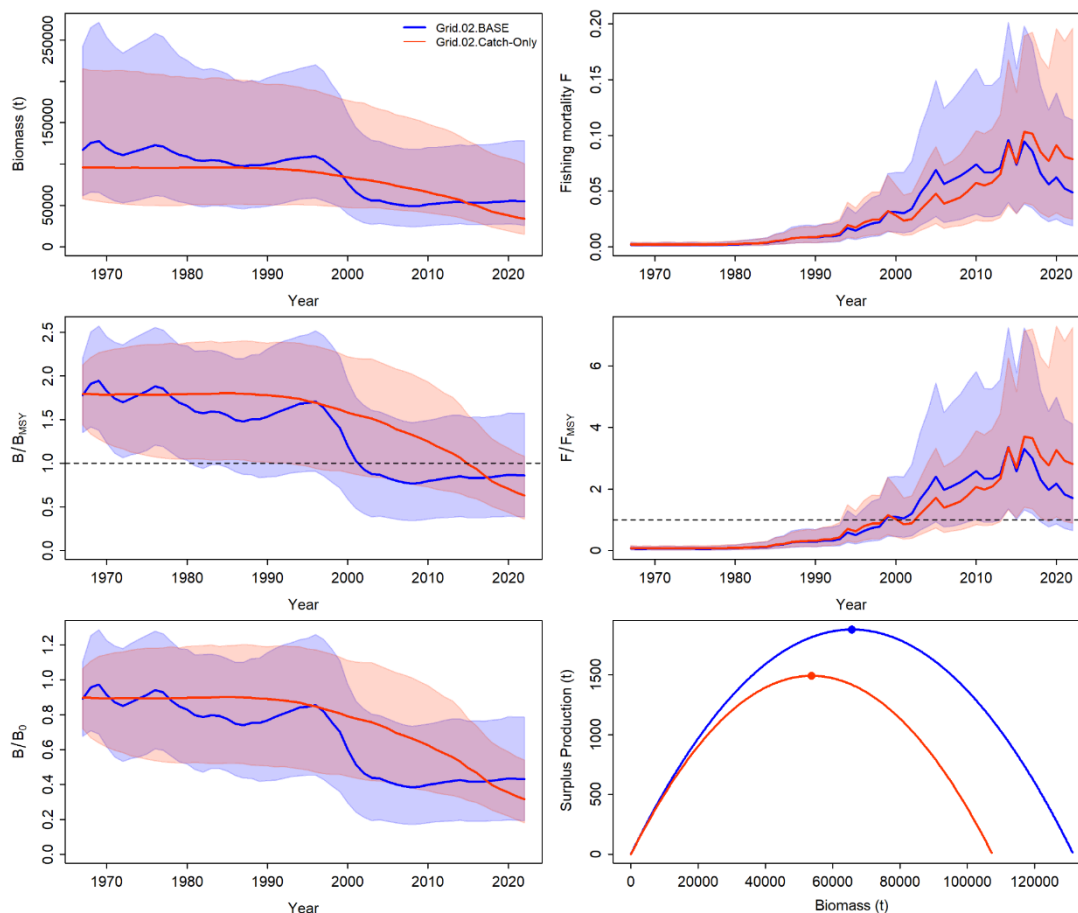

Figure 11: Sensitivity analysis relative to a catch only model for the 2024 IOTC SMA stock assessment. The analysis was carried out in relation to the base case grid model 02. The sensitivities are shown relative to the variations in the time series of biomass, fishing mortality, biomass relative to BMSY, fishing mortality relative to FMSY, depletion (B/B0) and form of the surplus production function.

3.5.2. Leave-one-out CPUE

A second sensitivity analysis was conducted with leave-one-out CPUE scenarios, where each model was run excluding one CPUE series at each time, either starting with the full model using all CPUEs or the base case model. The main results are represented in **Figures 12** and **13**.

In the case of starting with the full model, it is noted that the CPUE series that has the largest effect in biomass and fishing mortality is the CPUE series from Japan. Without this series there is very little data from the period where the catches and fishing mortality started to increase in the middle period of the fishery, and therefore the biomass cannot

get information on the trends for that period. As for the remaining CPUE series, all have some effects especially in the middle period of the fishery, but with lower effects than seen with the Japanese series, and all provide similar results in the terminal year, especially with regards to F/Fmsy.

With regards to the sensitivities carried out in the base case models for the CPUE series (**Figure 12**), it is noticeable especially the importance of the Japanese series to inform the stock trends over the middle period, and the Spanish trends over the more recent period. If any of those series are removed from the base case models, the stock trajectories and end results would be very different. The USSR series is more important in the initial fishery period, but is much less influential in the end results with regards to the current stock status.
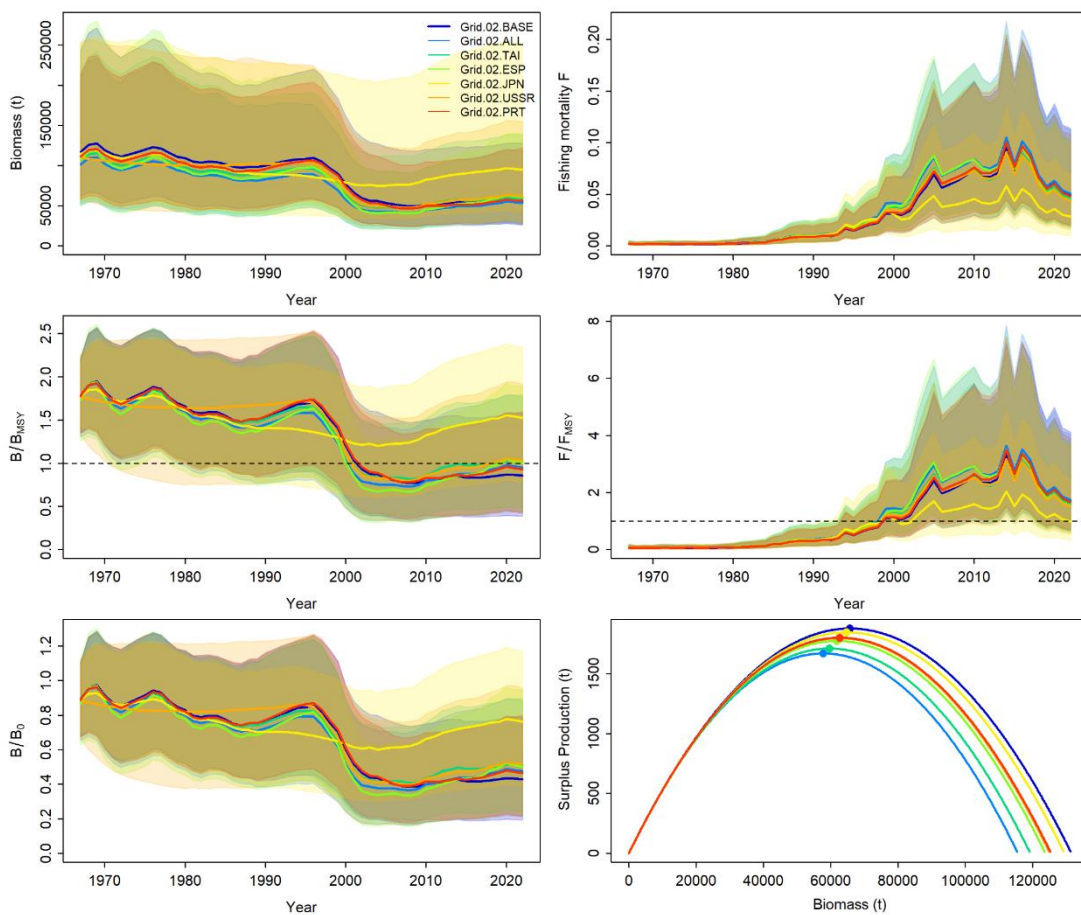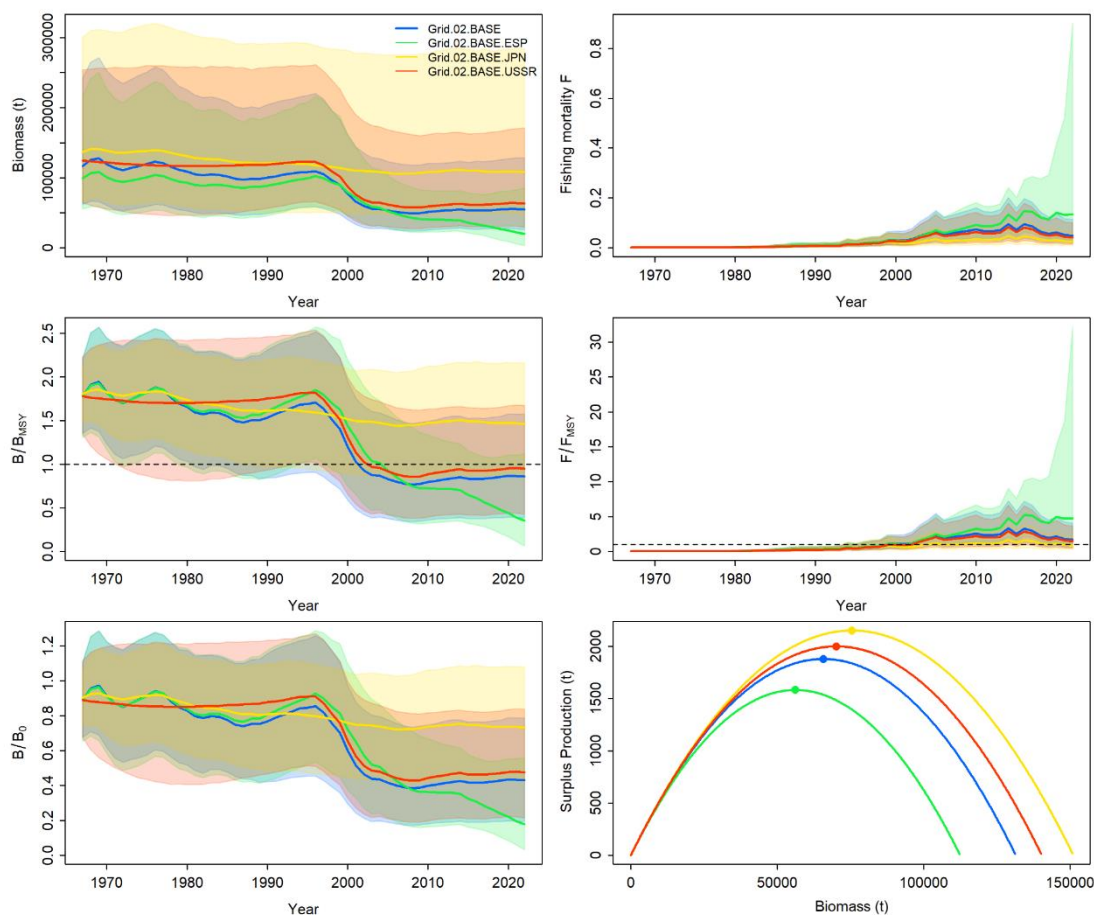

Figure 12: Sensitivity analysis relative to the leave-one-out CPUE series, performed for the 2024 IOTC SMA stock assessment. The analysis was carried out in relation to the configurations of the base case grid model 02, but using a full model using all CPUEs. The sensitivities are shown relative to the variations in the time series of biomass, fishing mortality, biomass relative to BMSY, fishing mortality relative to FMSY, depletion (B/B0) and form of the surplus production function.

Figure 13: Sensitivity analysis relative to the leave-one-out CPUE series, performed for the 2024 IOTC SMA stock assessment. The analysis was carried out in relation to the configurations of the base case grid model 02, using only the CPUEs from the base case models. The sensitivities are shown relative to the variations in the time series of biomass, fishing mortality, biomass relative to BMSY, fishing mortality relative to FMSY, depletion (B/B0) and form of the surplus production function

3.5.4. Process error and CPUE variance

Additional sensitivity analyses were carried out with regards to the process error and additional estimation of CPUEs variance. In the base case model the process error is estimated within the models with uninformative igamma priors, and the option to allow for additional CPUEs variance internally in JABBA is also allowed.

Sensitivities were run for options on fixing the sigma of the process error to CVs of 5% and 10%, and another to turn off the additional inclusion of CPUE variance. The results of this analysis are presented in **Figure 14**.

By fixing the process error to lower values the trajectories are much more stable and will result in less pessimistic stock status for the terminal year. The main caveat with this

option is related to the model validation procedures, as using such configuration results in worse model fit, with poorer fits to the CPUEs and worse performance in terms of retrospective analysis. In general, it is preferable to allow the process error to be estimated internally by the models, as that will optimize the posterior of the process error based on the rest of the data that is providing information to the models.

With regards to the additional CPUE variance, when that option is disabled, there are also very significant differences with the base case model, as the trajectories are forced to track the CPUEs much more closely. The biomass remains at similar levels in the initial period but with much more variability, and then drops considerably more when the fishing mortality increases around the years 2000's. The stock status at the end period is much more pessimistic, with much lower B/Bmsy and higher F/Fmsy than the base case models.
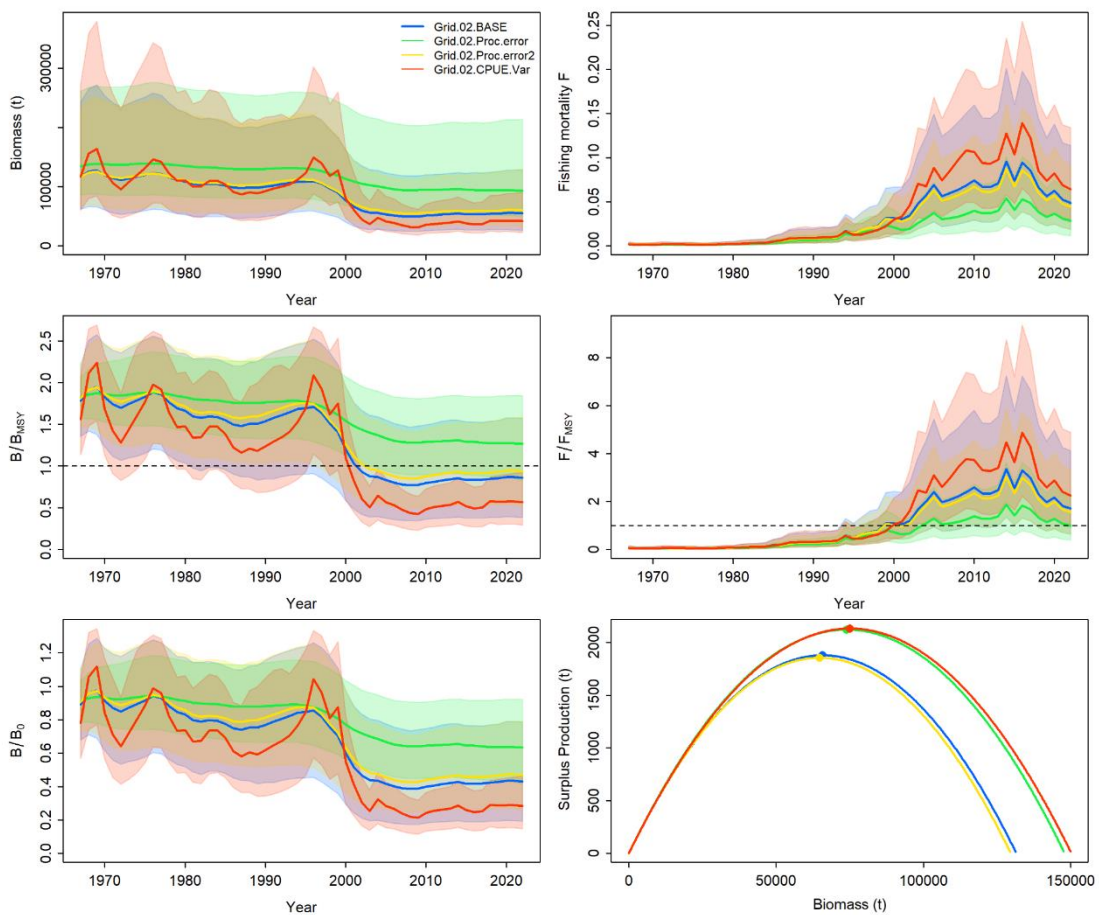

Figure 14: Sensitivity analysis relative to various options for the sigma of the process error ("BASE" = using an igamma vaguely informative prior; "proc.error" = fixing at 5%; "proc.error2" = fixing at 10%) and estimation of additional CPUE variance in the models, performed for the 2024 IOTC SMA stock assessment. The analysis was carried out in relation to the base case grid model 02. The sensitivities are shown relative to the variations in the time series of biomass, fishing mortality, biomass relative to BMSY, fishing mortality relative to FMSY, depletion (B/B0) and form of the surplus production function.

3.5.4. Using estimated catches

A final sensitivity analysis was conducted for using the estimated instead of reported catches, as reported in this paper. The main results of this analysis are represented in **Figure 15**.

In this case, the estimated catch series are at levels higher than the reported catch, and therefore there is a direct effect in terms of total stock biomass and overall MSY estimates. Also, given that the estimated catches continue to increase along the entire time series while in the reported catches there is a decrease in the more recent years, the fishing mortality for this alternative catch history also continues to increase and the end status for the relative biomass and fishing mortality is also much worse than in the base case models. Nonetheless, the depletion level and relative biomass at the end of the time series is similar to the base case model using reported catches.
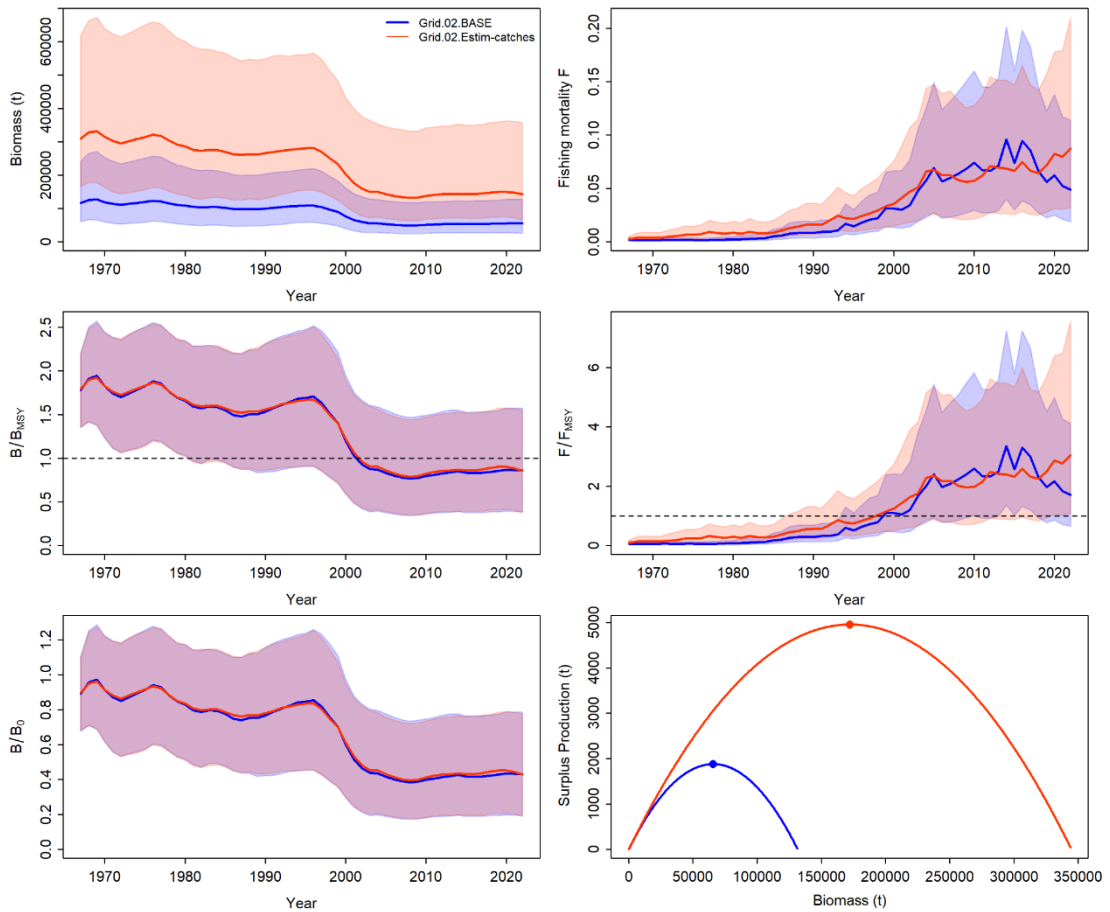

Figure 15: Sensitivity analysis relative to the catches using the ratio-based method, performed for the 2024 IOTC SMA stock assessment. The analysis was carried out in relation to the base case grid model 02. The sensitivities are shown relative to the variations in the time series of biomass, fishing mortality, biomass relative to BMSY,

fishing mortality relative to FMSY, depletion (B/B0) and form of the surplus production function.

3.6. Stock Status

The base case grid model trajectories of both biomass and fishing mortality in relation to MSY reference points are indicated in **Figure 16**. In general, it is noted that most of the grid models used have a current (2022) Fishing Mortality that is higher than Fmsy, with those values having a median value of 1.65, and ranging from 0.79 to 3.44. On the other hand, the status relative to biomass is more variable and dependent on specific models, with some grid models showing current (2022) biomass below Bmsy and others showing that current biomass is still above Bmsy. Specifically, the B/Bmsy of the base case grid had a median value of 0.96, ranging from 0.76 to 1.20. Those main trajectories of interest from the base case grid model in relation to absolute and relative biomass and fishing mortality are represented jointly in the plots in **Figure 17**.

The Kobe phase plots represented in **Figure 18** summarize those trends in the trajectories, with most of the models being either in the red or orange quadrants of the Kobe space, denoting therefore the current fishing mortality levels tend to be higher than those that support MSY, and that in most cases biomass is below Bmsy levels.
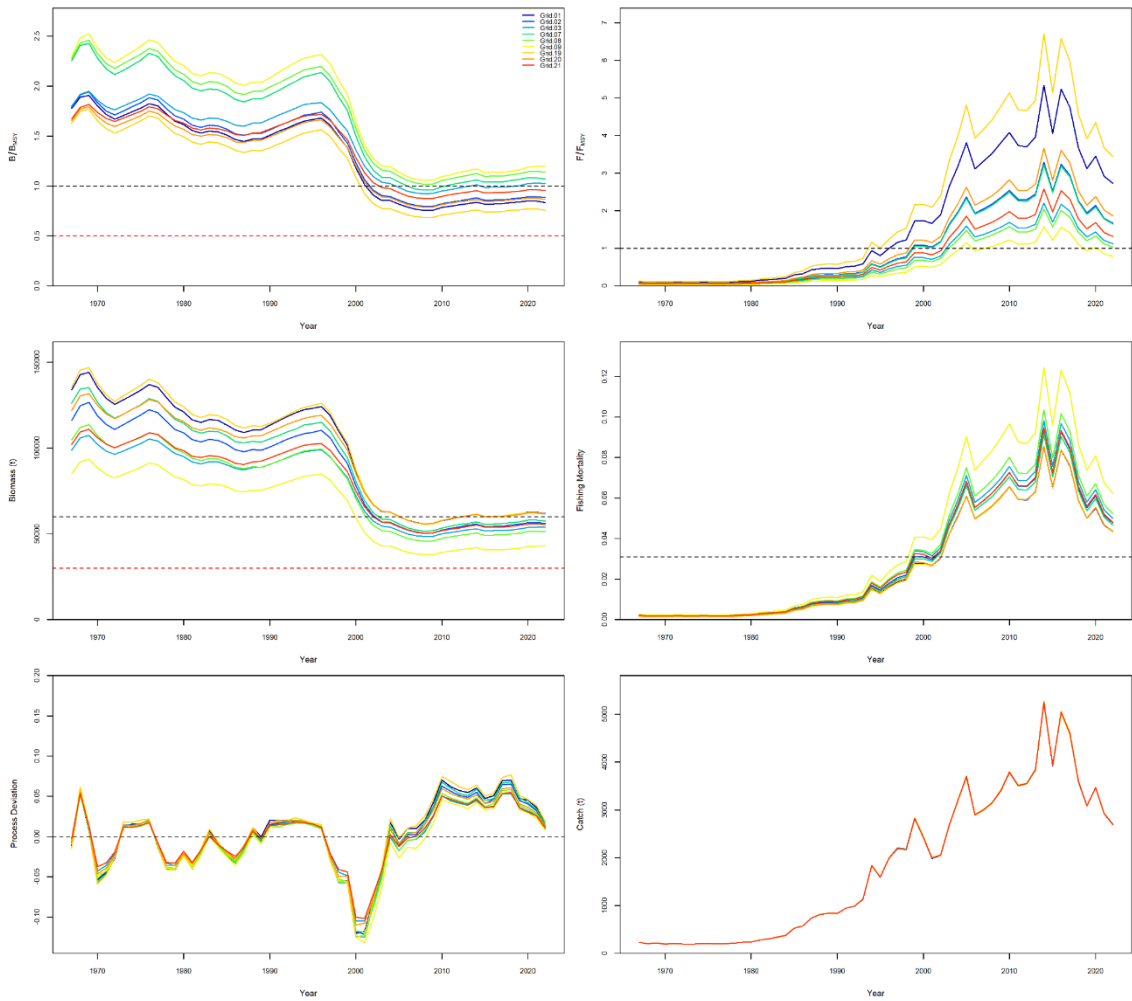
Figure 16: Trends of relative Biomass and Fishing Mortality in relation to MSY (Bmsy and Fmsy, respectively) for the base case grid models run for the 2024 IOTC SMA stock assessment. Plots from the Process Deviations and catches are also represented.
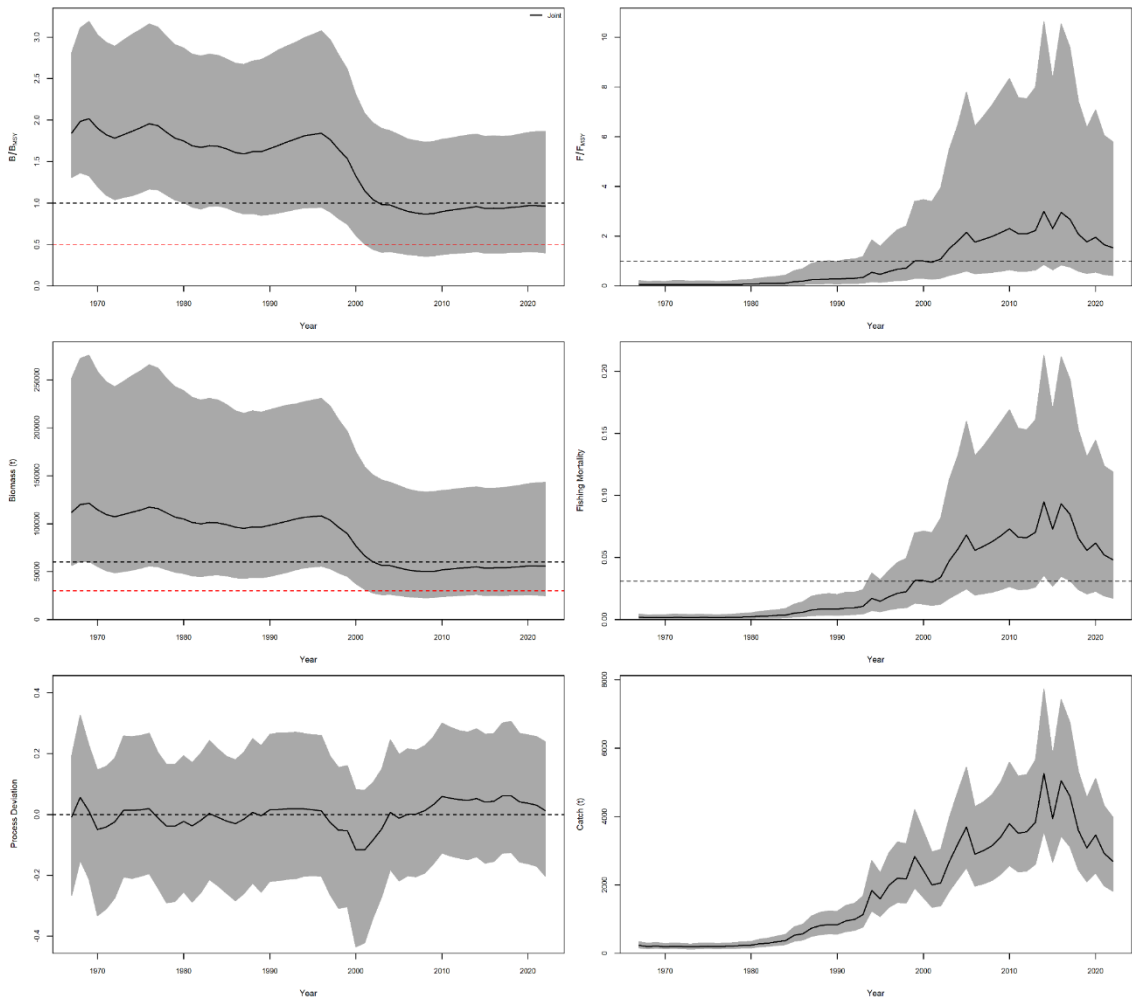
Figure 17: Trends of the joint trajectories of absolute and relative Biomass and Fishing Mortality (in relation to Bmsy and Fmsy, respectively) built from the base case grid models run for the 2024 IOTC SMA stock assessment. Plots from the Process Deviations and catches are also represented. All base case grid models are joint and plotted in a single line, with the respective 95% CIs.
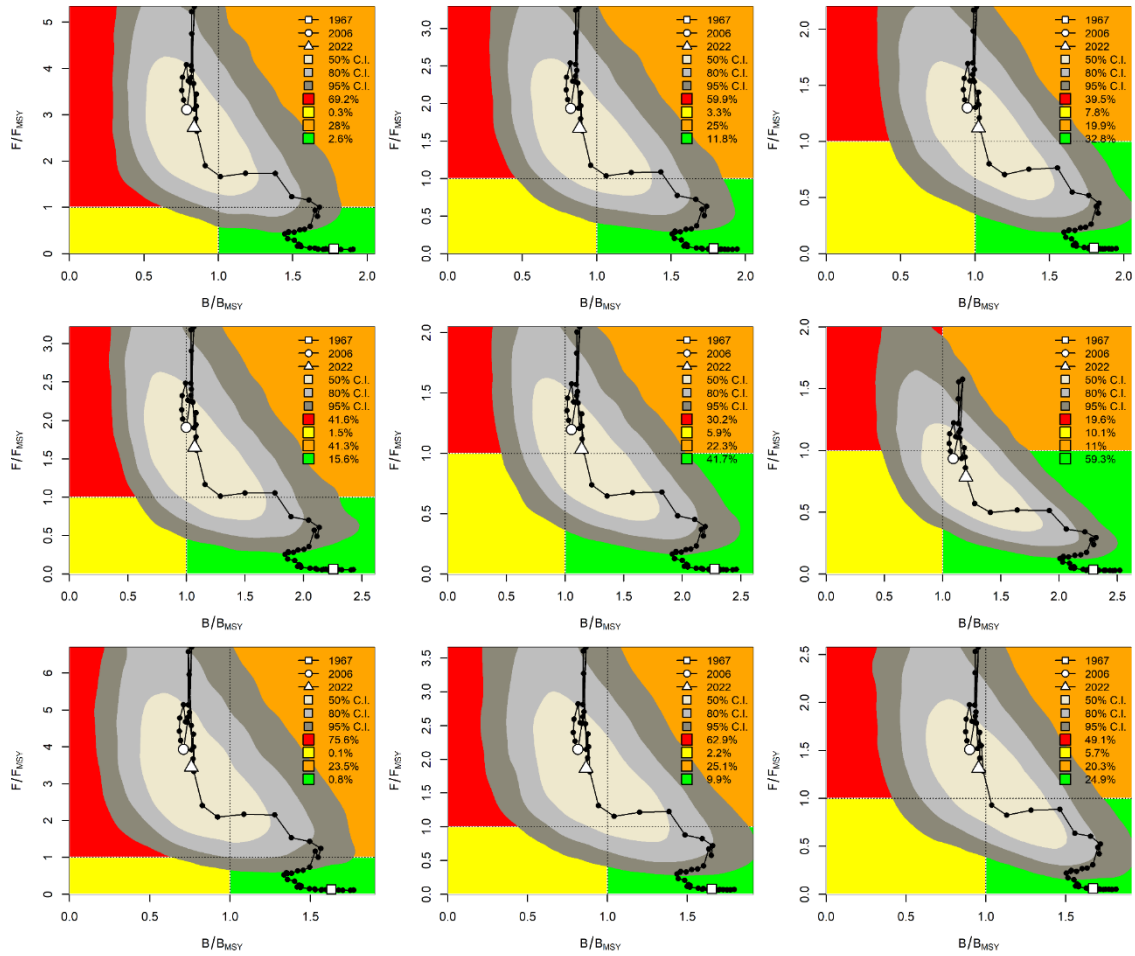
Figure 18: Kobe phase plot with the estimated trajectories (1967-2022) of B/Bmsy and F/Fmsy for the 2024 IOTC SMA stock assessment base case grid models. The different gray shaded areas denote the 50%, 80%, and 95% credibility intervals for the terminal year of the assessment data (2022). The probability of the terminal year stock status falling within each quadrant of the Kobe phase plot is indicated in the figure legend, for each of the grid models.

The overall and combined summaries of the main quantities of interest for the stock status from the ensemble grid models is presented in **Table 5**. The Kobe plot with the final year (2022) distribution of B/Bmsy and F/Fmsy for each of the grid models is represented in **Figure 19**. The combined Kobe plot for all base case grid models ensemble is represented in **Figure 20**. The probabilities of the stock in the final year (2022) being in each quadrant of the Kobe plot are represented in **Figure 21**.

The point estimates from the grid of stock assessment models shows that in 2022 the shortfin mako shark in the Indian Ocean was overfished (median B2022/Bmsy = 0.96, ranging between 0.79-1.20) and is undergoing overfishing (median F2022/Fmsy = 1.65, ranging between 0.79-3.44) (**Table 5**). The average MSY was estimated at 1,873.1 t, ranging between 1062.4 t and 2,949.6 t.

Considering the uncertainties explored, the probabilities (in percentage) of the stock being in each quadrant of the Kobe plot are 49.7% in the red (overfished and subject to overfishing), 24.0% in the orange (not overfished but subject to overfishing), 22.2% in the green (not overfished and not subject to overfishing) and 4.1% in the yellow (overfished but not subject to overfishing).

Table 5: Estimates (median, minimum and maximum) of the point estimates for Bmsy, Fmsy, MSY, B/Bmsy and F/Fmsy, from the 9 base case grid models used for the 2024 IOTC SMA stock assessment.

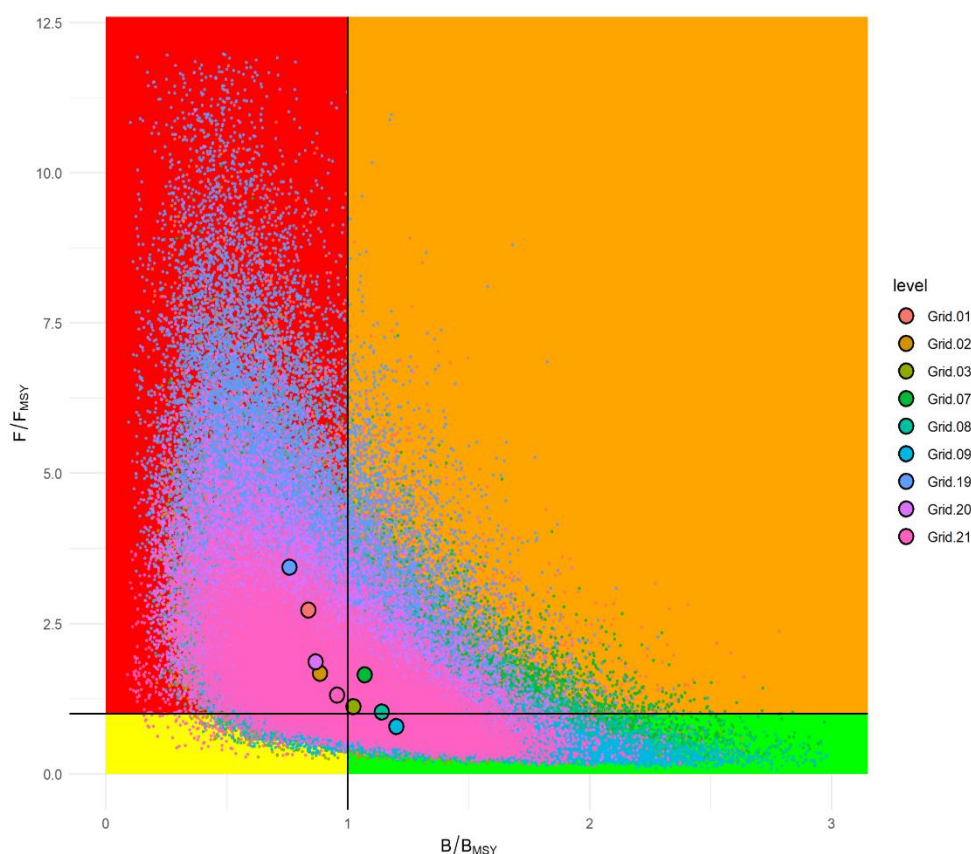| Parameter	Median	Min	Max
Fmsy	0.029	0.013	0.079
Bmsy	60999.64	37075.55	83147.99
MSY	1873.1	1062.4	2949.6
B2022/Bmsy	0.96	0.76	1.20
F2022/Fmsy	1.65	0.79	3.44

Figure 19: Kobe plot for the terminal year (2022) with the median point from the 9 base case grid models, used in the ensemble model grid approach for determining the stock status in the 2024 IOTC SMA stock assessment.
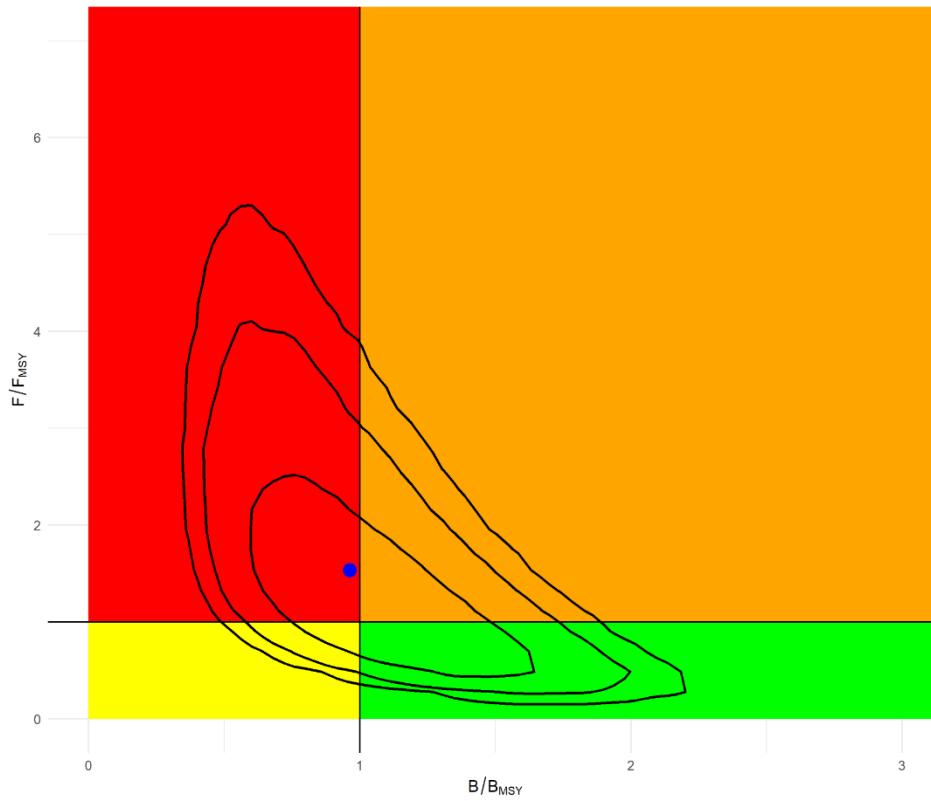
Figure 20: Kobe plot for the terminal year (2022) for all base case grid models combined, used for determining the stock status in the 2024 IOTC SMA stock assessment. The contour lines represent the 0.5, 0.8 and 0.9 quantiles of the distribution of the data.
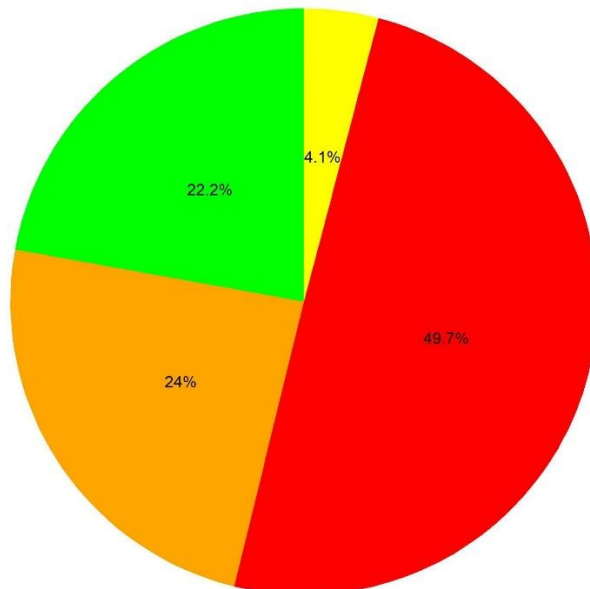

Figure 21: Probabilities (in percentage) of the IOTC shortfin mako shark stock being in each quadrant of the Kobe plot, from the combined base case model grid used.

3.7. Projections

The results for the stochastic projections from the 9 grid models ensemble in JABBA are represented in **Figure 22**. The main point to note is that current catches and respective fishing mortality are higher than Fmsy, while biomass is slightly below Bmsy and therefore there is a need to reduce catches or otherwise the biomass will continue to decline continuously.

The probabilities of violating the MSY-reference levels over 3, 10, 20 and 30-year periods, and considering various levels of future catches (TACs, established as percentages of current catches), are represented in **Table 6**.

A reduction of future catches to 40% of current catches, which would represent a constant annual catch (TAC) of 1,217.2 t per year, will have less than 50% probability of violating both MSY-reference points, i.e., to return the stock to the green quadrant of the Kobe plot in the next 10 years. Under such TAC (1,217.2 t), such probability of violating both MSY-reference points would be below 50% in 10 years, and would continue to decline over time, reaching values closer to 40% of violaging B/Bmsy, and 30% of violating F/Fmsy in a 30 year period.
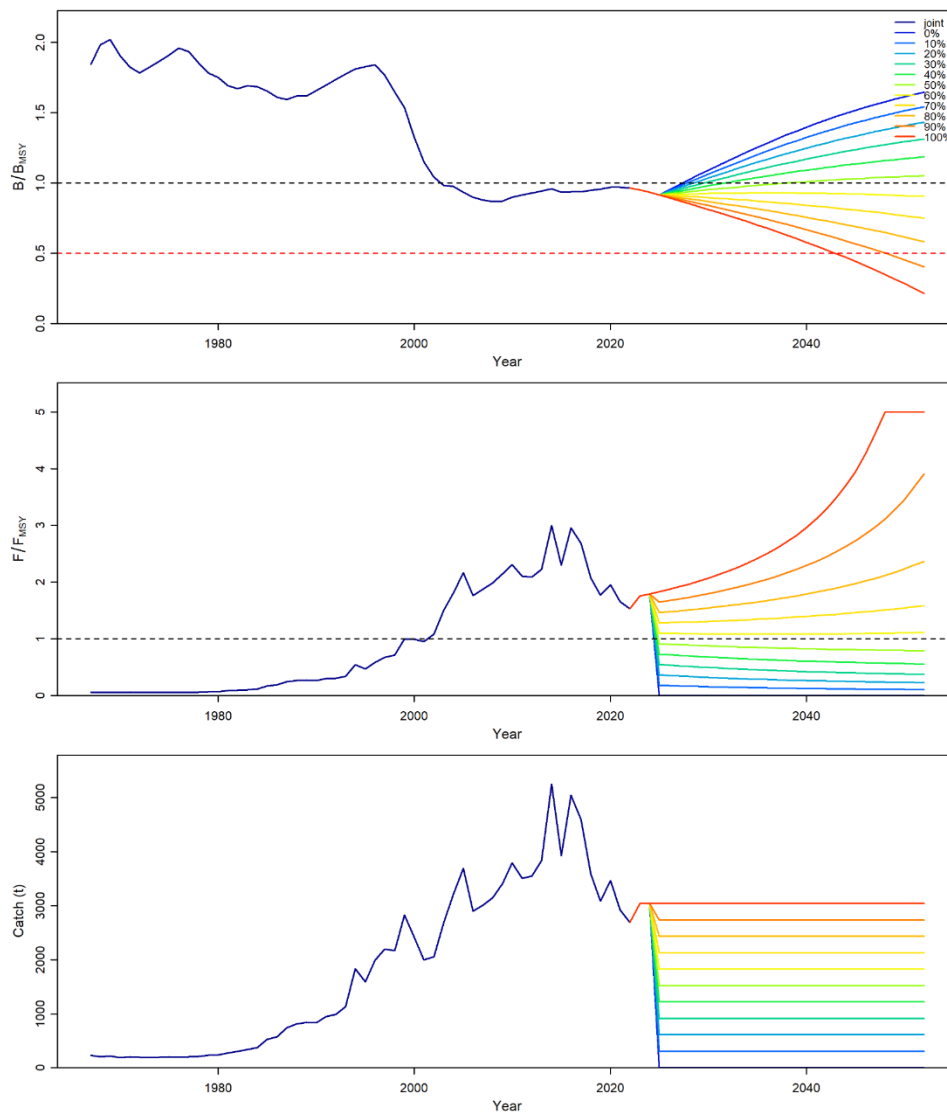
Figure 22: Joint trajectories and stochastic projections of B/Bmsy and F/Fmsy from the joint 9 base case grid model ensemble for the 2024 IOTC SMA stock assessment. The projections were run for a period of 30 years, with TACs (constant catches) ranging from 0% to 100% of current catches, with 10% increments. Current catches are defined as the average catches from the last 3-years (2020-2022: 3,042.9 t). Each line represents the median projections for B/Bmsy and F/Fmsy for each maximum catch (TAC) scenario. Note: these plots do not contain the respective CIs for simplification of the visualization.

Table 6: Shortfin mako aggregated IOTC Kobe II Strategy Matrix. The table shows the probabilities (in percentage) of violating the MSY-based reference points over the next 3, 10, 20 and 30 year periods. The projections are calculated for constant catches (0% to 100% of current catches, with 10% intervals) using the 9 base case model grid ensemble. The current catches are defined as the average of the last 3 years (average catch 2020-2022: 3042.9 t).

Reference point and projection time	Catch projections (relative to the 2020-2022 catches) and probability (%) of exceeding MSY-based reference points										
Catch relative to 2020-2022 (%)	0%	10%	20%	30%	40%	50%	60%	70%	80%	90%	100%
TAC (t)	0.0	304.3	608.6	912.9	1217.2	1521.5	1825.7	2130.0	2434.3	2738.6	3042.9
3 year projection											
B2025 < BMSY	57.7	57.7	57.7	57.7	57.7	57.7	57.7	57.7	57.7	57.7	57.7
F2025 > FMSY	0.0	1.5	9.6	21.7	34.1	45.3	55.1	63.2	70.0	75.7	80.2
10 year projection											
B2032 < BMSY	39.2	41.8	44.5	47.1	49.8	52.5	55.2	57.9	60.6	63.2	65.8
F2032 > FMSY	0.0	2.0	10.0	21.2	32.8	43.8	53.6	62.2	69.5	75.6	80.6
20 year projection											
B2042 < BMSY	26.1	30.0	34.4	39.1	44.0	49.0	54.1	59.1	64.0	68.6	72.9
F2042 > FMSY	0.0	2.4	10.2	20.6	31.9	42.8	52.9	62.0	69.9	76.5	81.8
30 year projection											
B2052 < BMSY	19.3	23.9	29.0	34.9	41.2	47.7	54.3	60.7	66.7	72.3	77.3
F2052 > FMSY	0.0	2.6	10.2	20.4	31.6	42.6	53.1	62.4	70.6	77.5	83.0

4. Conclusions (draft recommendation for management advice)

A Bayesian production model (JABBA) ensemble grid approach was used for determining the stock status and providing management advice for the Indian Ocean (IOTC) shortfin mako shark.

The models show that in 2022 the shortfin mako shark was overfished (median B2022/Bmsy = 0.96) and is undergoing overfishing (median F2022/Fmsy = 1.65), with an overall 49.7% probability.

Current catches (3042.9 t, average of 2020-2022) are too high to sustain the shortfin mako shark population above the MSY-reference levels over time. Such fishing mortality levels are currently higher than Fmsy, and will lead biomass to continue to decline to values further below Bmsy. In order to maintain the population above MSY-reference levels in the next 10-year period with at least a 50% probability, future catches (TACs) of the shortfin mako shark in IOTC should be no more than 1,217.2 t per year, which represents 40% of the current catches.

5. Acknowledgments

6. References

Anhøj, J., Olesen, A.V., 2014. Run charts revisited: A simulation study of run chart rules for detection of non-random variation in health care processes. *PLoS One*, 9: 1–13. https://doi.org/10.1371/journal.pone.0113825

Auguie, B., 2017. gridExtra: Miscellaneous Functions for "Grid" Graphics. R package version 2.3, https://CRAN.R-project.org/package=gridExtra.

Barreto, R.R., de Farias, W.K.T., Andrade, H., Santana, F.M., Lessa, R., 2016. Age, growth and spatial distribution of the life stages of the shortfin kako, *Isurus oxyrinchus* (Rafinesque, 1810) caught in the western and central Atlantic. *PLoS One*, 11 (4): e0153062.

Bonhommeau, S., Chassot, E., Barde, J., de Bruyn, P., Fiorellato, F., Nelson, L., Fu, D., Nieblas, A.E., 2020. Preliminary modelling for the stock assessment of shortfin mako shark, *Isurus oxyrinchus* using CMSY and JABBA. 16th Working Party on Ecosystems and Bycatch. 51 pp.

Brunel, T., Coelho, R., Merino, G., Ortiz de Urbina, J., Rosa, D., Santos, C., Murua, H., Bach, P., Saber, S., Macias, D. 2018. A preliminary stock assessment for the shortfin mako shark in the Indian Ocean using data-limited approaches. 14th Working Party on Ecosystems and Bycatch, 10-14 September, Cape Town, South Africa. IOTC Document, IOTC–2018–WPEB14–37. 19pp

Carnell R., 2022. triangle: Distribution Functions and Parameter Estimates for the Triangle Distribution. R package version 1.0, https://CRAN.R-project.org/package=triangle.

Carvalho, F., Punt, A.E., Chang, Y.J., Maunder, M.N., Piner, K.R., 2017. Can diagnostic tests help identify model misspecification in integrated stock assessments? *Fisheries Research*, 192: 28–40.

Carvalho, F., Winker, H., Courtney, D., Kapur, M., Kell, L., Cardinale, M., Schirripa, M., Kitakado, T., Yemane, D., Piner, K. R., Maunder, M. N., Taylor, I., Wetzel, C. R., Doering, K., Johnson, K. F., Methot, R. D. 2021. A cookbook for using model diagnostics in integrated stock assessments. *Fisheries Research*, 240: 105959.

Caswell, H., 2001. Matrix Population Models: construction, analysis, and interpretation, 2nd Edition. Sinauer Associates, Sunderland, Massachusetts.

Chen, S., Watanabe, S., 1989. Age dependence of natural mortality coefficient in fish population dynamics. *Nippon Suisan Gakkaishi*, 55: 205-208.

Coelho, R., Rosa, D. 2017. An alternative hypothesis for the reconstruction of time series of catches for North and South Atlantic stocks of shortfin mako sharks. Shortfin mako assessment meeting, 12-16 June 2017. Madrid, Spain. Collect. Vol. Sci. Pap. ICCAT, 74 (4): 1746-1758.

Coelho, R., Apostolaki, P., Bach, P., Brunel, T., Davies, T., Díez, G., Ellis, J., Escalle, L., Lopez, J., Merino, G., Mitchell, R., Macias, D., Murua, H., Overzee, H., Poos, J.J., Richardson, H., Rosa, D., Sánchez, S., Santos, C., Séret, B., Urbina, J.O., Walker, N. 2019. Improving scientific advice for the conservation and management of oceanic sharks and rays. Final Report. European Commission. Specific Contract No. 1 under Framework Contract No. EASME/EMFF/2016/008. 620 pp + Annexes. DOI: 10.2826/229340. Available at: https://publications.europa.eu/en/publication-detail/-/publication/bb27e867-6185-11e9-b6eb-01aa75ed71a1/language-en

Cortés, E., 2017. Estimates of maximum population growth rate and steepness for shortfin makos in the North and South Atlantic Ocean. ICCAT Document. SCRS/2017/126.

Gelman, A., 2006. Prior distributions for variance parameters in hierarchical models. *Bayesian Analysis*, 1(3): 515–533.

Gelman, A., Rubin, D.B., 1992. Inference from iterative simulation using multiple sequences. *Statistical Science*, 7, 457–472. https://doi.org/10.1214/ss/1177011136.

Geweke, J., 1992. Evaluating the accuracy of sampling-based approaches to the calculation of posterior moments. In: Berger, J.O., Bernardo, J.M., Dawid, A.P., Smith,A.F.M., (Eds.), Bayesian Statistics 4: Proceedings of the 4th Valencia International Meeting. Clarendon Press, Oxford, pp. 169–193.

Groeneveld, J.C., Cliff, G., Dudley, S.F.J., Foulis, A.J., Santos, J., Wintner, S.P., 2014. Population structure and biology of shortfin mako, *Isurus oxyrinchus*, in the south-west Indian ocean. Marine and Freshwater Research, 65: 1045-1058.

Heidelberger, P., Welch, P.D., 1992. Simulation run length control in the presence of an initial transient. *Operations Research*, 31. DOI: 1109–1144. https://doi.org/10.1287/opre.31.6.1109.

Hoenig, J.M., 1983. Empirical use of longevity data to estimate mortality rates. *Fishery Bulletin*, 82: 898-903.

Højsgaard S., Halekoh., U., 2023. doBy: Groupwise Statistics, LSmeans, Linear Estimates, Utilities. R package version 4.6.20, https://CRAN.R-project.org/package=doBy.

Hurtado-Ferro, F., Szuwalski, C.S., Valero, J.L., Anderson, S.C., Cunningham, C.J., Johnson, K.F., Licandeo, R., McGilliard, C.R., Monnahan, C.C., Muradian, M.L., Ono, K., Vert-Pre, K.A., Whitten, A.R., Punt, A.E., 2014. Looking in the rear-view mirror: Bias and retrospective patterns in integrated, age-structured stock assessment models. *ICES Journal of Marine Science*, 99–110. https://doi.org/10.1093/icesjms/fsu198.

Huynh, H.H., Hung, C-Y., Tsai, W-P., 2022. Demographic analysis of shortfin mako shark (*Isurus oxyrinchus*) in the South Pacific Ocean. *Animals*, 12(22), 3229. https://doi.org/10.3390/ani12223229.

Huynh, H.H., Tsai, W-P., 2023. Exploring the spatio-temporal dynamics of standardized CPUE for shortfin mako shark (*Isurus oxyrinchus*) caught by the Taiwanese large-scale tuna longline fishery in the Indian Ocean. IOTC Paper, WPEB.

Jensen, A.L., 1996. Beverton and Holt life history invariants result from optimal trade-off of reproduction and survival. *Canadian Journal of Fisheries and Aquatic Sciences*, 53: 820-822.

Kell, L.T., Sharma, R,. Winker, H., 2022. Artefact and artifice: evaluation of the skill of Catch-Only methods for classifying stock status. *Frontiers in Marine Science*, 9: 762203. doi: 10.3389/fmars.2022.762203.

Liu, K-M. Sibagariang, R.D., Joung, S-J., Wang, S-B., 2018. Age and growth of the shortfin mako shark in the southern Indian Ocean. *Marine and Coastal Fisheries: Dynamics, Management, and Ecosystem Science*, 10: 577–589.

Martell, S., Froese, R., 2013. A simple method for estimating MSY from catch and resilience. *Fish and Fisheries*, 14: 504–514.

Myers, R.A., Bowen, K.G., Barrowman, N.J., 1999. Maximum reproductive rate of fish at low population sizes. *Canadian Journal of Fisheries and Aquatic Sciences*, 56: 2404–2419.

Mollet, H.F., Cliff, G., Pratt, H.L., Stevens, J.D., 2000. Reproductive biology of the female shortfin mako, *Isurus oxyrinchus* (Rafinesque, 1810), with comments on the embryonic development of lamnoids. *Fishery Bulletin*, 98: 299–318.

Mollet, H.F., Cailliet, G.M., 2002. Comparative population demography of elasmobranchs using life history tables, Leslie matrices and stage-based matrix models. *Marine and Freshwater Research*, 53: 503–516.

Mourato, B., Sant'Ana, R., Kikuchi, E., Cardoso, L.G., Ngom, F., Arocha, F., Kimoto, A., Ortiz, M., 2023. Assessment of the eastern Atlantic sailfish stock using JABBA model. *Collective Volumes of Scientific Papers ICCAT*, 80(8): 315-336.

Murua, H., Abascal, F.J., Amande, J., Ariz, J., Bach, P., Chavance, P., Coelho, R., Korta, M., Poisson, F., Santos, M.N., Seret, B. 2013. EUPOA-Sharks: Provision of scientific advice for the purpose of the implementation of the EUPOA sharks. Studies for Carrying out the Common Fisheries Policy; Reference: MARE/2010/11Final Report. European Commission. 443 pp.

Murua, H., Santiago, J., Coelho, R., Zudaire, I., Neves, C., Rosa, D., Zudaire, I., Semba, Y., Geng., Z., Bach, P., Arrizabalaga, H., Bach, P., Baez, J.C., Ramos, M.L., Zhu, J.F., Ruiz, J., 2018. Updated Ecological Risk Assessment (ERA) for shark species caught in fisheries managed by the Indian Ocean Tuna Commission (IOTC). IOTC Document, IOTC-2018-SC21-14_Rev1.

Natanson, L.J., Kohler, N.E., Ardizzone, D., Cailliet, G.M., Wintner, S.P., Mollet, H.F., 2006. Validated age and growth estimates for the shortfin mako, *Isurus oxyrinchus*, in the North Atlantic Ocean. Environmental Biology of Fishes, 77: 367–83.

Pauly, D., 1980. On the interrelationships between natural mortality, growth parameters, and mean environmental temperatures in 175 fish stocks. *Journal du Conseil International pour l'Exploration de la Mer*, 39: 175-192.

Peterson, I., Wroblewski, J.S., 1984. Mortality rates of fishes in the pelagic ecosystem. *Canadian Journal of Fisheries and Aquatic Sciences*, 41: 1117-1120.

Plummer, M., 2003. JAGS: A Program for Analysis of Bayesian Graphical Models using Gibbs Sampling, 3rd International Workshop on Distributed Statistical Computing (DSC 2003); Vienna, Austria.

Plummer, M., Nicky, B., Cowles, K., Vines, K., 2006. CODA: convergence diagnosis and output analysis for MCMC. *R News*, 6 (1): 7–11.

R Core Team, 2023. R: A Language and Environment for Statistical Computing. R Foundation for Statistical Computing, Vienna, Austria. https://www.R-project.org/.

Romanov, E., Romanova, N. 2009. Size distribution and length-weight relationships for some large pelagic sharks in the Indian Ocean. 5th WPEB, 12-14 October 2009, Mombasa, Kenya. IOTC document IOTC2009-WPEB-06. 12 pp.

Rosa, D., Mas, F., Alyssa, M., Natanson, L.J., Domingo, A., Carlson, J., Coelho, R.,2017. Age and growth of shortfin mako in the North Atlantic, with revised parameters for consideration to use in the stock assessment. 2017 ICCAT Shortfin mako assessment meeting, 12-16 June 2017, Madrid, Spain. ICCAT document SCRS/2017/111: 22 pp.

Simpfendorfer, C.A., 2004. Demographic models: life tables, matrix models and rebound potential. *In* Elasmobranch fisheries management techniques (Musick, J. A. & Bonfil, R., eds.), pp. 187-204. Singapore: APEC.

Stevens, M.H.H., 2009. A Primer of Ecology with R (2nd printing), Springer, New York.

Stubben, C.J., Milligan, B.G., 2007. Estimating and analyzing demographic models using the popbio package in R. *Journal of Statistical Software*, 22(11). doi:10.18637/jss.v022.i11.

Su, Yajima., 2012. R2jags-a package for running jags from R. https://cran.r-project.org/web/packages/R2jags/index.html

Takahashi, N., Kai, M., Semba, Y., Kanaiwa, M., Liu, K-M., Rodríguez-Madrigal, J.A., Tovar-Ávila, J., Kinney, M.J., Taylor, J.N., 2017. Meta-analysis of growth curve for shortfin mako shark in the North Pacific. ISC Shark Working Group Workshop, 28 November – 4 December 2017, NRIFSF Shimizu, Shizuoka, Japan.

Tsai, W-P., Liu, K-M., Punt, A.E., Sun, C-L., 2015. Assessing the potential biases of ignoring sexual dimorphism and mating mechanism in using a single-sex demographic model: the shortfin mako shark as a case study. *ICES Journal of Marine Scienc*e, 72 (3): 793–803. https://doi.org/10.1093/icesjms/fsu210

Winker, H., Carvalho, F., Kapur, M., 2018. JABBA: Just Another Bayesian Biomass Assessment. *Fisheries Research* 204, 275–288. https://doi.org/http://doi.org/10.1016/j.fishres.2018.03.01.

Wickham, H., 2007. Reshaping data with the reshape package. *Journal of Statistical Software*, 21(12), 2007.

Wickham, H. 2016. ggplot2: Elegant Graphics for Data Analysis. Springer-Verlag, New York.

Wickham, H., Averick, M., Bryan, J., Chang, W., McGowan, L.D., François, R., Grolemund, G., Hayes, A., Henry, L., Hester, J., Kuhn, M., Pedersen, T.L., Miller, E., Bache, S.M., Müller, K., Ooms, J., Robinson, D., Seidel, D.P., Spinu, V., Takahashi, K., Vaughan, D., Wilke, C., Woo, K., Yutani, H., 2019. Welcome to the tidyverse. *Journal of Open Source Software*, 4 (43): 1686. doi:10.21105/joss.01686.

Wickham, H., François, R., Henry, L., Müller, K., Vaughan, D., 2023. dplyr: A Grammar of Data Manipulation. R package version 1.1.4, https://CRAN.R-project.org/package=dplyr.

Wickham, H., Vaughan, D., Girlich, M., 2023. tidyr: Tidy Messy Data. R package version 1.3.0, https://CRAN.R-project.org/package=tidyr.

Wilke, C., 2024. cowplot: Streamlined Plot Theme and Plot Annotations for 'ggplot2'. R package version 1.1.3, https://CRAN.R-project.org/package=cowplot

Yokoi, H., Ijima, H., Ohshimo, S., Yokawa, K., 2017. Impact of biology knowledge on the conservation and management of large pelagic sharks. *Scientific Reports*, 7: 10619.